

Subtle dimensions of climate change have strong
demographic effects on a cactus population in
extinction debt

Kevin Czachura and Tom E.X. Miller*

Program in Ecology and Evolutionary Biology, Department of
BioSciences, Rice University, Houston, TX USA

*Corresponding author: tom.miller@rice.edu (1-713-348-4218)

Abstract

- 1 1. The effects of climate change on population viability reflect the net influ-
2 ence of potentially diverse responses of individual-level demographic pro-
3 cesses (growth, survival, regeneration) to multiple components of climate.
4 Articulating climate-demography connections can facilitate forecasts of re-
5 sponses to future climate change as well as back-casts that may reveal how
6 populations responded to historical climate change.
- 7 2. We studied climate-demography relationships in the cactus *Cyclindriopun-*
8 *tia imbricata*; previous work indicated that our focal population has high
9 abundance but a negative population growth rate, where deaths exceed
10 births, suggesting that it persists under extinction debt. We parameter-
11 ized a climate-dependent integral projection model with data from a 14-year
12 field study, then back-casted expected population growth rates since 1900
13 to test the hypothesis that recent climate change has driven this population
14 into extinction debt.
- 15 3. We found clear patterns of climate change in our central New Mexico study
16 region but, contrary to our hypothesis, *C. imbricata* has most likely bene-
17 fitted from recent climate change and is on track to reach replacement-level
18 population growth within 38 years, or sooner if climate change accelerates.
19 Furthermore, the strongest feature of climate change (a trend toward years
20 that are overall warmer and drier, captured by the first principal component
21 of inter-annual variation) was not the main driver of population responses.
22 Instead, temporal trends in population growth were dominated by more sub-

23 tle, seasonal climatic factors with relatively weak signals of recent change
24 (wetter and milder cool seasons, captured by the second and third principal
25 components).

26 4. *Synthesis*. Our results highlight the challenges of forecasting population dy-
27 namics under climate change, since the most apparent features of climate
28 change may not be the most important drivers of ecological responses. Envi-
29 ronmentally explicit demographic models can help meet this challenge, but
30 they must consider the magnitudes of different aspects of climate change
31 alongside the magnitudes of demographic responses to those changes.

32 **Keywords**

33 Cactaceae; Climate change; Demography; Extinction debt; Integral Projection
34 Model; Long-term ecological research

Introduction

Population extinction debt is likely to increase in frequency as a fingerprint of global change, including climate change (Dullinger *et al.*, 2012; Urban, 2015). Extinction debt is a form of transient dynamics whereby populations persist despite having population growth rates that fall below replacement level ($\lambda < 1$), suggesting a long-term trajectory toward local extinction but with potentially long time lags (Hastings *et al.*, 2018; Kuussaari *et al.*, 2009). While extinction debt is often studied through species richness patterns at the community level (e.g., Vellend *et al.* 2006), there is recent emphasis on the underlying single-species dynamics whereby populations transition from positive to negative growth rates (Lehtilä *et al.*, 2016; Hylander & Ehrlén, 2013). In the absence of significant migration (which can maintain populations in sink habitats), extinction debt suggests that the environment was more favorable for population growth at some time in the past. However, the mechanisms that cause populations to tip from positive to negative growth rates are rarely known, and this information may be critical for effective conservation planning (Hylander & Ehrlén, 2013).

Structured population models built from individual-level demographic rates provide a powerful framework for studying drivers of extinction debt (Lehtilä *et al.*, 2016) and environment-dependent population dynamics more generally (Ehrlén & Morris, 2015). By incorporating climatic factors as statistical covariates, previous studies have identified climatic limits of population viability and forecasted responses to particular types of climate change (e.g., Adler *et al.* 2013; Maschinski *et al.* 2006; Jenouvrier *et al.* 2014). Additionally, articulating the connections between environment and demography can allow for ‘back-casting’ popu-

59 lation dynamics into historical environmental regimes; while rarely done (Smith
60 *et al.*, 2005), this approach may provide valuable insight regarding when and why
61 populations fell into extinction debt.

62 Many studies of climate-demography relationships focus on single climate vari-
63 ables that are known to be a dominant component of climate change and / or
64 known to have a strong influence on the focal species (e.g., Van de Pol *et al.* 2010;
65 Iler *et al.* 2019; Jenouvrier *et al.* 2009). However, for many species, it is not always
66 apparent *a priori* which dimensions of climate are most important, and this poses
67 challenges for predicting population responses to climate change. Previous studies
68 have shown that different components of climate change may have independent
69 effects on different aspects of demography or physiology (Buckley & Kingsolver,
70 2012; Frederiksen *et al.*, 2008; Van de Pol *et al.*, 2010; Lynch *et al.*, 2014). Fur-
71 thermore, different life stages (e.g., young vs old) and different vital rate processes
72 (e.g., growth, survival, reproduction) may differ in the magnitude and even di-
73 rection of their responses to single climate drivers (Doak & Morris, 2010; Dybala
74 *et al.*, 2013; Morrison & Hik, 2007; Tenhumberg *et al.*, 2018), and single life stages
75 or vital rates may be affected by multiple drivers (Dalglish *et al.*, 2011; Williams
76 *et al.*, 2015; Frederiksen *et al.*, 2008; Sletvold *et al.*, 2013). Ultimately, the influ-
77 ence of climate on population growth depends on the sensitivities of vital rates
78 to climate drivers and the sensitivities of λ to the vital rates, integrated across the
79 life cycle (McLean *et al.*, 2016; Ådahl *et al.*, 2006). These complications, common
80 to environmentally explicit demographic studies (Ehrlén *et al.*, 2016), highlight
81 the value of leveraging long-term data to gain resolution of climate drivers and the
82 importance of accounting for demographic complexity across the life cycle.

83 We used long-term demographic data to study climate-dependent population

84 dynamics of a long-lived Chihuahuan desert cactus persisting under extinction
 85 debt. Our previous work with the tree cholla cactus (*Cylindriopuntia imbricata*
 86 Haw. D.C.) (Cactaceae) indicated, with >95% certainty, that our focal population
 87 in the northern Chihuahuan Desert (New Mexico, USA) is in decline (stochastic
 88 population growth rate $\lambda_S < 1$) despite current densities that are reasonably high
 89 (Ohm & Miller, 2014; Miller *et al.*, 2009; Elderd & Miller, 2016). This region has
 90 experienced strong climatic fluctuations over the past century, including several
 91 decadal-scale droughts interrupted by relatively wet periods (Peters *et al.*, 2015).
 92 Recent and projected climate change in our study region includes increases in
 93 temperature and shifts in the seasonal timing of precipitation (Petrie *et al.*, 2014;
 94 Cook & Seager, 2013; Cook *et al.*, 2015).

95 Our study was conducted in the following steps. First, we characterized climate
 96 variation and change in our northern Chihuahuan desert study region over the past
 97 century. Second, we estimated vital rate responses to inter-annual climate vari-
 98 ation during the demographic study period (2004–2017). We hypothesized that
 99 high-sensitivity vital rates (those that strongly influence λ) would be less respon-
 100 sive environmental variability than low-sensitivity vital rates (Pfister, 1998). Third,
 101 we back-casted climate-dependent demography to determine whether the past cen-
 102 tury included periods that were favorable for population growth, thus testing the
 103 hypothesis that recent climate change has driven this population into extinction
 104 debt. Our analysis relied on a Bayesian framework that incorporates key sources
 105 of uncertainty into our back-cast. Finally, we asked whether the components of
 106 climate that are changing most strongly are the same climate components that
 107 most strongly influence cactus demography.

Materials and methods

Focal species, study site, and demographic data collection

Tree cholla cactus is widely distributed throughout desert and grassland habitats of the southwest U.S. and northern Mexico. These long-lived plants (40-plus years) grow through the production and elongation of cylindrical stem segments. These vegetative structures as well as flowerbuds are initiated in late spring. Flowering occurs in early summer and stem segment elongation takes place during the remainder of the growing season. For climate analyses, we divide the calendar year into warm-season months (May through September), when stem elongation, flowering, and seed production occur, and cool-season months (October through April).

This study was conducted at the Sevilleta National Wildlife Refuge (SNWR), a Long-Term Ecological Research site (SEV-LTER) in central New Mexico and near the center of this species' geographic distribution. Our study population occurs in the Los Piños mountains at an elevation of 1790 m. Tree cholla are a dominant component of the vegetation in this area (0.1 m^{-2} : Miller *et al.* 2009), along with oaks, yucca, Piñon pine, and the grasses *Bouteloua gracilis* and *B. eriopoda*.

The present study relies on long-term (2004–2017) demographic data on individual-level measures of growth, survival, and reproduction recorded from tagged plants in the Los Piños population that were censused in late May each year. This was a pre-breeding census that corresponds to the initiation of vegetative and reproductive structures (Fig. C1). We treat May 1 as the start of the transition year (coincident with the start of the warm-season months). There were a total of 1172 unique individuals in the data set and 7442 transition-year observations from 4–8

plots or spatial blocks depending on the year. Full details of the study design and data collection are given elsewhere (Miller *et al.*, 2009; Ohm & Miller, 2014; Elder & Miller, 2016).

Climate data

Our goal was to connect inter-annual variation in demography to corresponding variation in temperature and precipitation. SEV-LTER collects climate data from a network of meteorological stations throughout SNWR, with the oldest records coming from the late 1980s. While the SEV-LTER climate data cover years of our demographic data collection, our intention was to back-cast demographic performance farther back into the 20th century. We therefore gathered climate data from ClimateWNA v5.60 (Wang *et al.*, 2016), a software package that uses PRISM (Daly *et al.*, 2008) and WorldClim (Hijmans *et al.*, 2005) data to calculate downscaled data for western North America based on location and elevation, going as far back as 1900. We derived seasonal estimates (warm- and cool-season) of total precipitation and mean, minimum, and maximum temperature from monthly climate data, for a total of eight variables. Months were aligned to correspond to demographic transition years rather than calendar years, which means the cool-season climate for a transition year beginning in May of year t spans October of year t through April of year $t + 1$ (Fig. C1).

To reduce the dimensionality of the climate data, we conducted Principal Components Analysis (PCA) on the eight climate variables for the years 1900-2017, with climate values scaled to unit variance. We estimated the variance in the raw climate data explained by each PC and the variable loadings, which give the cor-

relations between original variables and PC values. PCA allowed us to rank the magnitudes of multiple aspects of climate variation and change by examining how warm- and cool-season variables loaded onto the ranked PC axes.

By relying on downscaled, interpolated climate data instead of direct observations from meteorological stations we are trading off local resolution in favor of more historical years of data. We quantified this loss of resolution by comparing predictions from ClimateWNA to SEV-LTER data for years that they over-lapped, using the SEV-LTER meteorological station that was nearest our study population (Appendix A). We found that the two data sets were generally well correlated (Table A1, Fig. A1,A2), which bolstered our confidence in ClimateWNA for back-casting demographic responses to climate over the historical record. We further explored the implications of using downscaled data by repeating all our analyses SEV-LTER meteorological data and comparing results between the two data sources (Appendix A).

Statistical estimation of climate-dependence

We fit generalized linear mixed effects models in a hierarchical Bayesian framework to quantify climate dependence in demographic vital rates, as captured by three principal components of climatic variability. The choice of three PCs was based on results of parallel analysis (Fig. A3), a statistical method for determining how many components to retain (Franklin *et al.*, 1995). There were four vital rates measured in the long-term study for which we could estimate climate dependence: survival from year t to year $t+1$, individual growth (change in size from year t to year $t+1$), probability of flowering in year t , and the number of flowerbuds

178 produced year in t , given that a plant flowered. Survival and growth from year $t-1$
 179 to t were dependent on size in year $t-1$, and the climate covariate corresponded
 180 to the climate year $t-1$ to t . Reproductive status and fertility in year t were
 181 dependent on size in year t and on climate from $t-1$ to t . This timing of size
 182 and climate effects was intended to match processes in the population model (Fig.
 183 C1). We did not quantify climate-dependence in seedling recruitment. While we
 184 searched plots each year and added newly detected plants to the census, we could
 185 not confidently assign a birth year to these new additions (seedlings require several
 186 years of growth before they are consistently detectable in our census) so we do not
 187 know the climatic conditions under which they recruited.

188 All of the models for climate-dependent vital rates used the same linear predic-
 189 tor for the expected value (μ) but applied a different link function ($f(\mu)$) depending
 190 on the distribution of the observations:

$$\begin{aligned}
 f(\mu) = & \beta_0 + \beta_1 x + \\
 & \rho_1^1 PC1 + \rho_2^1 PC1^2 + \rho_3^1 x PC1 + \\
 & \rho_1^2 PC2 + \rho_2^2 PC2^2 + \rho_3^2 x PC2 + \\
 & \rho_1^3 PC3 + \rho_2^3 PC3^2 + \rho_3^3 x PC3 + \\
 & \gamma + \tau
 \end{aligned} \tag{1}$$

191 The linear predictor includes a grand mean intercept (β_0) and size-dependent
 192 slope (β_1). The size variable x is the natural logarithm of plant volume ($\log_e(cm^3)$),
 193 which was standardized to mean zero and unit variance for analysis. Other fixed-
 194 effect coefficients (ρ) correspond to climate variables and climate \times size inter-

actions. We include quadratic terms for climate to account for the possibility of non-monotonic climate responses. Climate coefficient (ρ) superscripts correspond to each PC, and subscripts correspond to linear, quadratic, and size-interaction effects. Finally, the linear predictor includes normally distributed random effects for plot-to-plot variation ($\gamma \sim N(0, \sigma_{plot})$) and year-to-year variation that is unrelated to climate effects captured by PCs 1-3 ($\tau \sim N(0, \sigma_{year})$). The year random-effect can be interpreted as inter-annual variability in demography that cannot be explained by the climate PCs. We used stochastic variable selection in a Bayesian framework to reduce model complexity, dropping coefficients that were effectively zero with $\geq 90\%$ certainty. Complete methods for variable selection are provided in Appendix B.

The growth data were normally distributed; this model applied the identity link and included an additional parameter for residual variance. We explored size-dependence in the residual variance of growth (which determines how individuals are distributed around their expected future size) but found that this led to poorer model fits, so we proceeded to assume a constant value. The survival and flowering data were Bernoulli distributed, and these models applied the logit link function. The fertility data (flowerbud counts) were modeled as Poisson-distributed, including an individual-level random effect to account for overdispersion. All coefficients were given vague priors. We evaluated model fits using posterior predictive checks (Elder & Miller, 2016). All models were fit using JAGS (Plummer *et al.*, 2003) and R2JAGS (Su & Yajima, 2012). Analysis code is available at https://github.com/texmiller/cholla_climate_IPM.

Demographic modeling

Model description

The statistical models described above formed the backbone of the integral projection model (IPM) that we used to estimate population growth in variable climate environments. Following previous studies (Compagnoni *et al.*, 2016; Ohm & Miller, 2014; Elderd & Miller, 2016), we modeled the life cycle of *C. imbricata* using continuously size-structured plants, $n(x)$, and two discrete seed banks ($B_{1,t}$ and $B_{2,t}$) corresponding to 1 and 2-year old seeds:

$$B_{1,t+1} = \kappa \delta \int_L^U P(x, \mathbf{c}_{t-1}; \alpha_t^P) F(x, \mathbf{c}_{t-1}; \alpha_t^F) n(x)_t dx \quad (2)$$

$$B_{2,t+1} = (1 - \gamma_1 B_{1,t}) \quad (3)$$

Functions P and F give the probability of flowering and the number of flower-buds produced, respectively, for an x -sized plant. The vector \mathbf{c}_{t-1} contains the climate PC values for climate-year $t - 1$, which affects flowering and fertility in year t , and hence the 1-year old seed bank in year $t + 1$. Parameters α_t^P and α_t^F are random year effects estimated from the statistical models. The integral is multiplied by the number of seeds per fruit (κ) and probability of seed dispersal/survival (δ) to give the number of seeds that enter the 1-year old seed bank. Parameters L and U are the lower and upper bounds, respectively, of the plant size distribution. Plants can recruit out of the 1-year old seed bank with probability γ_1 or transition to the 2-year old seed bank with probability $(1 - \gamma_1)$. Seeds in the 2-year old seed bank are assumed to either germinate (probability γ_2) or die.

237 Continuous-size dynamics were given by:

$$n(y)_{t+1} = (\gamma_1 B_{1,t} + \gamma_2 B_{2,t})\eta(y)\omega + \int_L^U S(x, \mathbf{c}_t; \alpha_t^S)G(y, x, \mathbf{c}_t; \alpha_t^G)n(x)_t dx \quad (4)$$

238 The first term indicates recruitment from the seed banks to size y , where $\eta(y)$
 239 gives the seedling size distribution, assumed normal with mean μ_s and standard
 240 deviation σ_s . Mortality between germination (late summer) and the yearly demo-
 241 graphic census (May) is accounted for with survival probability ω . In the second
 242 term, functions S and G give the probabilities of surviving to year $t+1$ and grow-
 243 ing to size y , respectively, for an x -sized plant in year t . Climate-dependence and
 244 random year effects are included as in Eq. 2, except the timing of climate effects
 245 is shifted such that growth and survival from t to $t+1$ are affected by climate over
 246 the same interval (Fig. C1). As above, survival and growth functions also take
 247 time-varying random intercepts. Field data used to estimate seed and seed bank
 248 parameters are described elsewhere (Compagnoni *et al.*, 2016; Elderd & Miller,
 249 2016). All parameter estimates are provided in Table C1.

250 Model analysis

251 For analysis, we discretized x into n bins, replacing the continuous kernel with an
 252 n -by- n matrix (because our model also included two additional discrete states, the
 253 final projection matrix had dimensions $n+2$ -by- $n+2$). We used $n = 200$ bins. We
 254 extended integration limits L and U to avoid unintentional “eviction” (Williams
 255 *et al.*, 2012).

256 We estimated the asymptotic population growth rate λ as the dominant eigen-

257 value of the discretized IPM kernel. We compared the observed size distribution
 258 and the predicted distribution at the long-term mean climate ($PC_1 = PC_2 =$
 259 $PC_3 = 0$) and found generally good agreement (Fig. C2). We then evaluated how
 260 λ responded to climate variation by first varying each climate PC independently,
 261 holding the other two fixed at their long-term mean. Second, we back-casted λ
 262 over the entire climatological record that we had available (1900–2017), which gen-
 263 erated a time series of λ_t . We used linear regression to test for temporal trends
 264 in λ over this period. We incorporated two types of uncertainty into back-casted
 265 values of λ : imperfect knowledge of the parameter values (“estimation error”) and
 266 year-to-year fluctuations that were not related to climate (“process error”); the
 267 latter was estimated from the variances of random year effects. For the years of
 268 demographic data collection (2004–2017), we additionally quantified the deviations
 269 between predicted λ based solely on climate and “observed” λ that reflects climate
 270 and non-climate year effects (quotations indicate that these are the asymptotic pre-
 271 dictions given the vital rates observed in that year). We also conducted a similar
 272 analysis of λ_S using a 10-year sliding window (Appendix C), and we explored the
 273 consequences of extrapolating vital rate responses to climate values more extreme
 274 than those observed during the study period (Appendix D).

Finally, we used Life Table Response Experiments (LTREs) to decompose
 which combinations of climate PCs and vital rate responses were most strongly
 responsible for temporal fluctuations in the back-casted time series λ_t . We used
 a fixed-design LTRE (Caswell, 2001) where λ_t was defined as a linear function of

climate predictors:

$$\lambda_t = \bar{\lambda} + \sum_{i=1}^3 \gamma_i PC_{i,t} \quad (5)$$

There is no error term because, in this analysis, climate PCs are assumed to be the sole drivers of fluctuations in λ_t . The coefficient for each climate PC was approximated as:

$$\gamma_i \approx \sum_{j=1}^n \frac{\partial \bar{\lambda}}{\partial \theta_j} \frac{\partial \theta_j}{\partial PC_i} \quad (6)$$

275 The LTRE approximation is based on the product of the sensitivity of λ to the vital
 276 rates (θ), evaluated at the long-term mean climate ($PC_1 = PC_2 = PC_3 = 0$), and
 277 the sensitivity of the vital rates to climate, summed over all vital rates n . Because
 278 LTRE components are additive, we summed LTRE estimates over the intercept
 279 and slope of each vital rate function so that we could interpret the results in terms
 280 of vital rate contributions.

281 Results

282 Climate trends

283 Three principal components cumulatively explained 73.3% of the inter-annual vari-
 284 ation in climate (Figure 1A). PC1 was dominated by inter-annual differences in
 285 temperature and precipitation, regardless of season, and the three components of
 286 temperature (mean, min, max) loaded similarly onto this component (Figure 1B).
 287 Over the last century, PC1 trends have fluctuated, with prolonged stretches of

288 warm and dry years (the 1950s and early 2000s) and other periods of cool and
289 wet years (early 1900s and 1970s-80s), though the overall temporal trend for PC1
290 is negative. The decline per-year is nearly five times stronger since 1970 com-
291 pared to the long-term average (Fig. 1C), suggesting an accelerating trajectory
292 of warmer and drier years. PC2 was strongly driven by cool-season climate, espe-
293 cially precipitation, such that greater values corresponded to wetter winters with
294 low temperature maxima and high temperature minima (Figure 1B). Warm-season
295 temperatures also loaded positively onto this axis to a lesser degree (Figure 1B).
296 PC2 has increased since 1900 and the change per-year is nearly four times stronger
297 since 1970 (Figure 1D), indicating an accelerating trend of wetter cool seasons with
298 moderate winter temperatures. Lastly, PC3 was correlated with a combination of
299 warm- and cool-season climate variables. The strongest variable loadings on this
300 component were minimum and mean temperatures in the cool season and warm-
301 season precipitation. Temporal trends for PC3 showed weak declines since 1900,
302 corresponding to milder winters with higher minimum and mean temperatures and
303 wetter warm seasons; this trend has been slightly stronger since 1970 (Figure 1E).

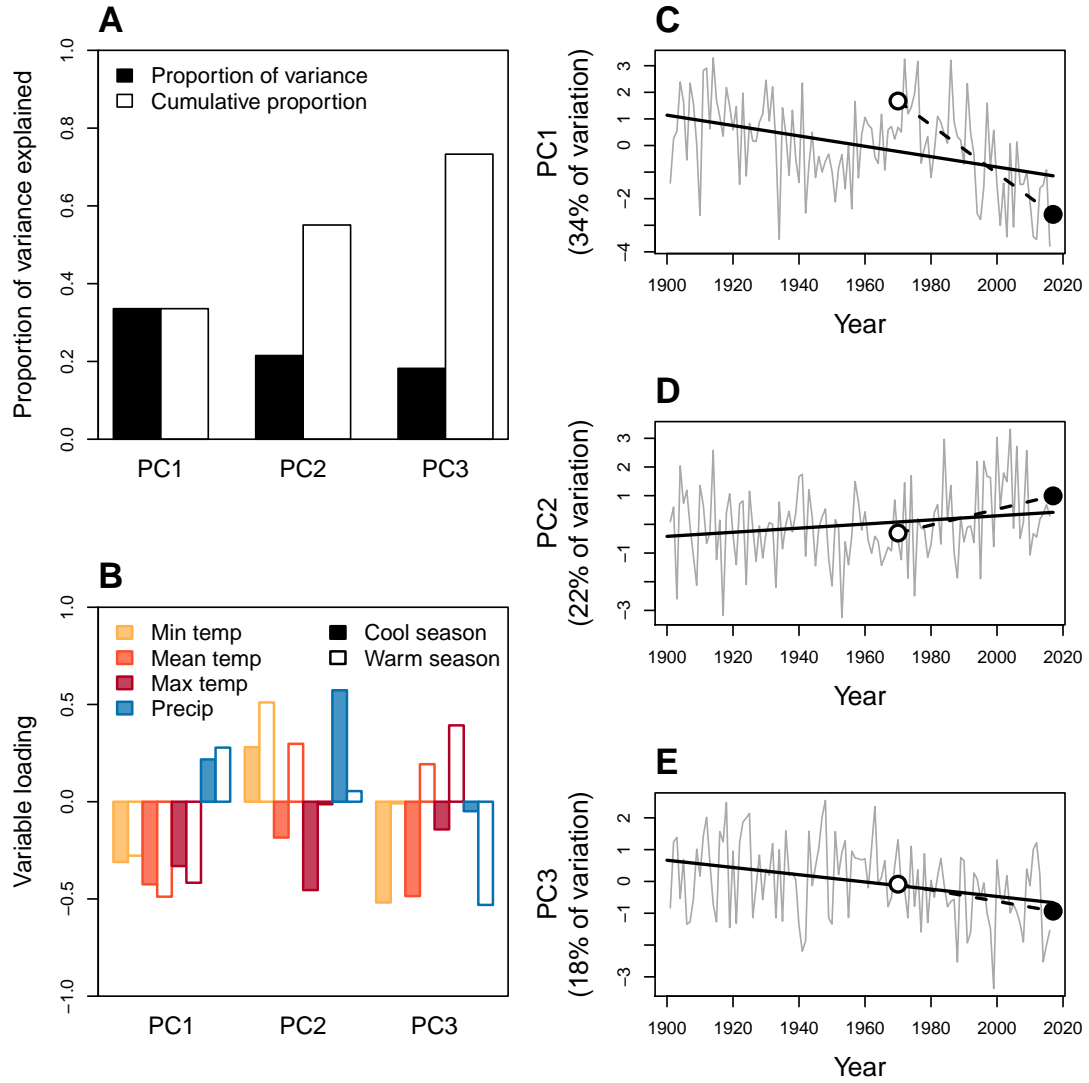


Figure 1: Principal components analysis (PCA) of inter-annual climate variability at SNWR, 1901–2017. **A**, Proportion and cumulative proportion of variation in seasonal temperatures (minimum, mean, maximum) and precipitation explained by the first three PCs. **B**, Loadings of seasonal climate variables onto PC1-3. Because climate data were standardized to mean zero and unit variance, loadings can be interpreted as the correlation between the climate variable and the PC. **C–E**, Time series of PC values, with regression lines showing long-term trends since 1901 (solid lines) or 1970 (dashed lines); open and filled points indicate the years 1970 and 2017, respectively, and correspond to the same shapes in Fig. 3

Vital rate responses to climate

Demographic vital rates estimated from long-term data (survival, growth, reproductive status, and fertility of flowering plants) were least responsive to PC1, the dominant axis of climate variability and change. All of the vital rates were strongly, positively size-dependent but there was heterogeneity in the magnitude and sign of responses to different dimensions of climate variability. Figure 2 shows vital rate data and fitted statistical models following variable selection procedures that eliminated coefficients that were weakly supported (Table B1). There was very little support for coefficients of quadratic climate effects (Table B1), indicating that responses to climate were monotonic over the range of variation we observed.

For PC1, there was a weak reduction in survival probability (especially for smaller plants; Fig. 2A) and a moderate reduction in flowering probability (especially for larger plants; Fig. 2G) at higher PC values, i.e., in cooler and wetter years. Fertility of flowering plants was not responsive to PC1 variation (Fig. 2J) and growth was not responsive to any of the climate PCs (Fig. 2D,E,F). There were positive responses to PC2 in survival (Fig. 2B), flowering probability (Fig. 2H), and fertility of flowering plants (Fig. 2K), indicating that these vital rates benefitted from years with wetter cool seasons. Responses to PC3 varied in sign, with survival increasing with decreasing PC values (years with mild winter temperature minima and wet summers) and reproductive rates increasing with increasing PC values (years with low winter minima and dry summers) (Fig. 2C,I,L).

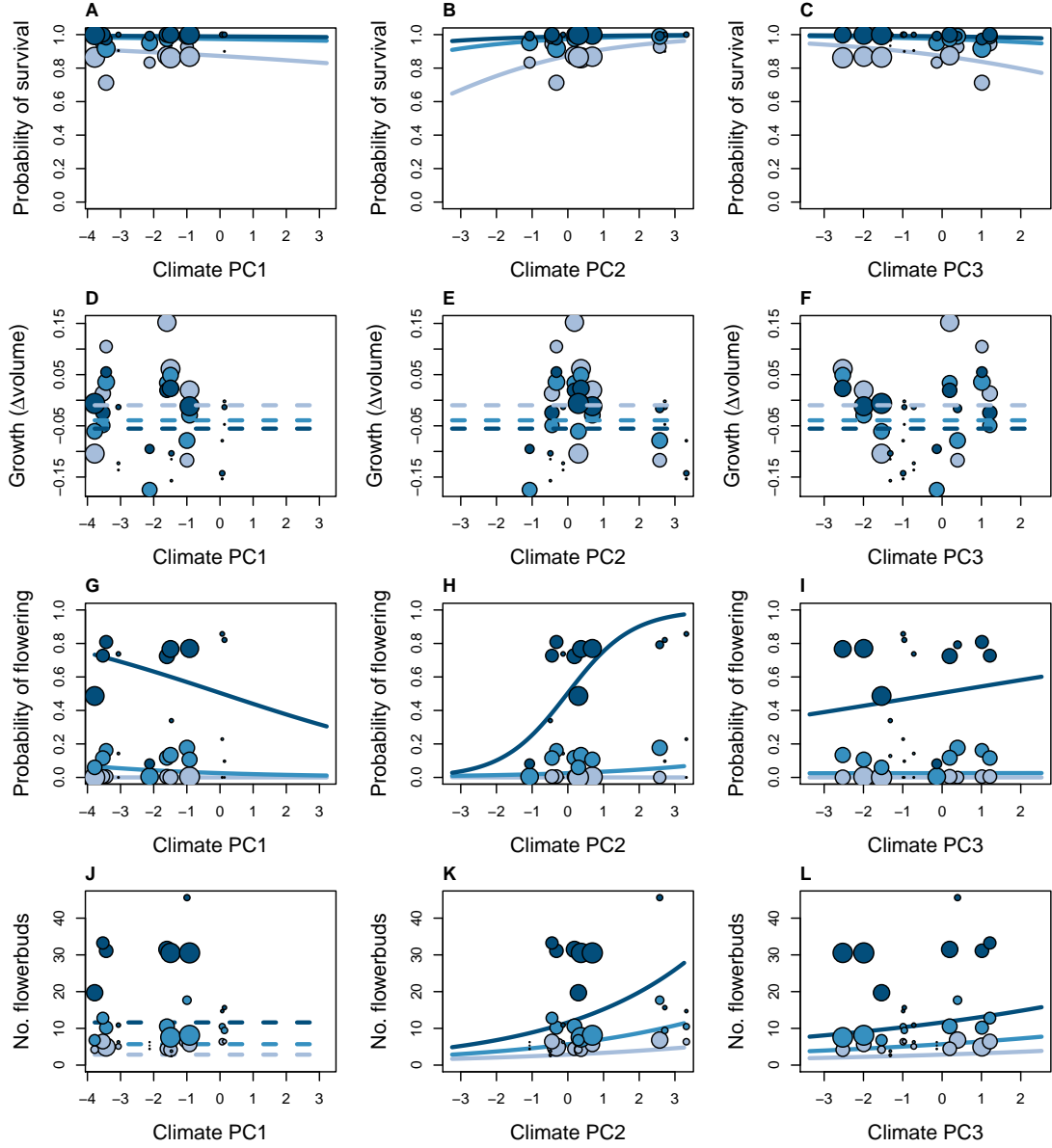


Figure 2: Climate- and size-dependent variation in survival (A-C), growth (D-F), flowering (G-I), and fertility of flowering plants (J-L) in relation to three principal components of seasonal climate variation (columns). For visualization only, the plant size distribution was discretized into three groups (small, medium, and large, corresponding to increasingly dark shading). Points show means for each size group in each year, where different years have unique PC values and point size is proportional to sample size for each size group in each year. Lines show fitted statistical models using posterior mean parameter values, with shading corresponding to size groups. Dashed lines indicate that the climate predictor was not statistically supported. Ranges of x -axes show the climate extrapolation that was required for back-casting.

Climate-dependent population growth

The population growth rate λ was predicted to increase with decreasing values of PC1 (hotter, drier years), holding other PCs fixed at their long-term average (Fig. 3A). Population growth was also predicted to increase with increasing values of PC2 (wetter cool seasons; Fig. 3B). Population growth was more sensitive to PC2 than PC1, such that the predicted change in λ from 1970 to 2017 was slightly greater for PC2 even though PC1 exhibited much greater change than PC2 over this period. Finally, greater values of PC3 (colder winters and drier summers) were predicted to cause declines in population growth, indicating that negative effects on cactus survival outweighed positive effects of PC3 on reproduction (Fig. 2). PC3 has changed relatively little since 1970 but this was associated with a change in λ of about half the magnitude to the response to relatively large change in PC1. Overall, recent climate change in each of the principal components, in isolation, has been in the direction that favors increased population growth (Fig. 1, 3). However, mean estimates for population growth rates were consistently below replacement level for all climate PC values, and the posterior probability densities rarely met or exceeded $\lambda = 1$.

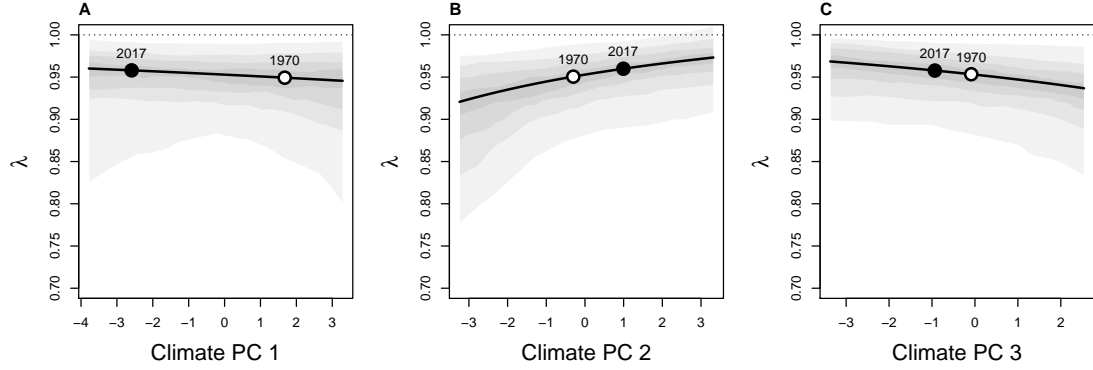


Figure 3: Predicted asymptotic population growth rate (λ) in response to three principal components of inter-annual climatic variation (A-C). For each panel, the indicated principal component is varying while the others are held at zero (the average value). Lines show the expected relationships based on posterior mean parameter values and shaded contours show the 25,50,75, and 95% credible intervals, representing uncertainty in demographic parameters. Points highlight the change the PC value (on the x -axis) between 1970 and 2017, based on the regression lines shown in Fig. 1, and the predicted corresponding change in λ (y -axis).

Back-casting population growth

Figure 4A shows the back-casted time series of λ accounting for inter-annual variation in all three PC components. For the observation years (2004-2017), the three climate PCs explained 60% of the inter-annual variation in λ (points in Fig. 4A). Thus, even with relatively strong climate-demography associations (Fig. 2), there was substantial uncertainty in our back-casted estimates of λ . The shaded region in Fig. 4A represents the combined uncertainty arising from heterogeneity in vital rates across years that could not be attributed to the climate PCs (process error) and imperfect knowledge of the underlying parameters (estimation error). In Appendix Fig. C3, we show that process error contributed the majority of the

352 total uncertainty.

353 Despite uncertainty in our back-cast, the results indicated that λ has likely
354 remained below replacement levels for more than a century; there was no evidence
355 that climate change drove this population into extinction debt. To the contrary,
356 there was a positive temporal trend ($\frac{\Delta\lambda}{\Delta Year} > 0$), suggesting a trajectory of increas-
357 ing population growth rates through time (Fig. 4B). There was wide uncertainty
358 in the rate of change but the posterior probability distribution indicated that it
359 was 2.5 times more likely that λ has increased than decreased. Furthermore, the
360 median rate of increase was 2.27 times greater since 1970 compared to the overall
361 trend since 1900 (Fig. 4B), corresponding to the acceleration of climate change
362 (Fig. 1). There was greater uncertainty in $\frac{\Delta\lambda}{\Delta Year}$ since 1970 because this estimate
363 was based on fewer years. Under the trajectory since 1970, population growth
364 was expected to reach the threshold of positive population growth ($\lambda = 1$) in the
365 year 2057 (Fig. 4C); accelerating climate change would advance this transition to
366 viable growth rates.

367 In Appendix D, we show that our inference that λ is likely increasing in response
368 to climate change holds even with a more conservative approach that does not
369 extrapolate vital rate responses beyond the climate extremes of the observation
370 years. Furthermore, in Appendix A, we show that year-specific estimates of λ
371 were correlated between models built with downscaled climate data versus on-site
372 meteorological measurements, for years in which they over-lapped (Fig. A7). This
373 suggests that our qualitative inference regarding the temporal trend in λ is robust
374 to the loss of resolution associated with downscaled climate data.

375 The stochastic population growth rate (λ_S) showed a similar trend of $\lambda_S < 1$
376 and increasing population growth rates over the past 120 years (Fig. C4). The

377 stochastic growth rate reveals the effects of multi-year climate events, such as the
 378 runs of good years in the 1940s and 2000s.

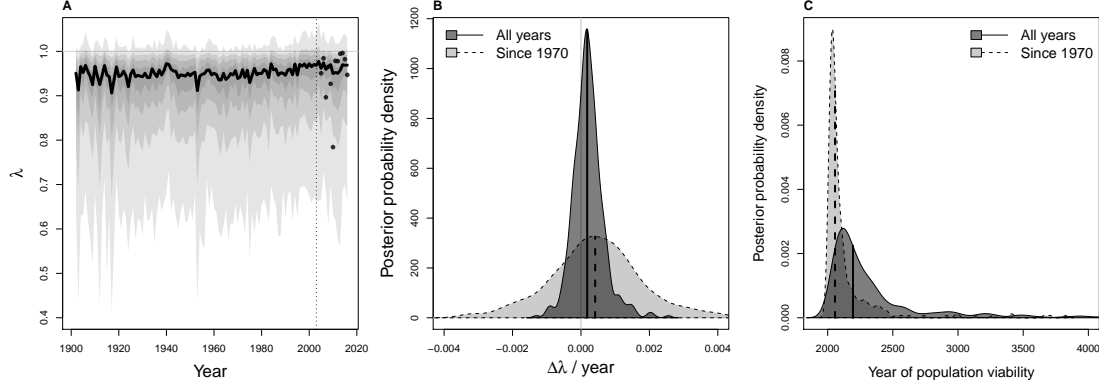


Figure 4: **A**, Posterior probability distribution for the time series of asymptotic population growth rates (λ) predicted based on inter-annual variation in three climate PCs. Thick black line shows the mean prediction and shaded regions show the 25, 50, 75, and 95% credible regions accounting for both parameter uncertainty and process error (year-to-year variation in vital rates that was unrelated to climate). Dashed vertical line separates years that were back-casted versus years that were directly observed. The observation years (2004 and later) include estimates for year-specific population growth rates (points), captured statistically as year-specific random effects in the vital rates. **B**, Posterior distributions for the rate of temporal change in population growth ($\frac{\Delta\lambda}{\Delta Y_{\text{ear}}}$). Dark grey shows the rate of change across all years shown in **A** and light grey shows the rate of change since 1970. Vertical lines show median values. **C**, Posterior distributions for the year of population viability ($\lambda = 1$) for the subset of posterior samples for which $\frac{\Delta\lambda}{\Delta Y_{\text{ear}}} > 0$. Shading and lines as in **B**.

379 Life Table Response Experiment

380 Life Table Response Experiments (LTRE) provided a decomposition of how λ
 381 responded to long-term climate trends (1900-2017), allowing us to understand the
 382 relative importance of different dimensions of climate variability and vital rate
 383 responses to them. LTRE results indicated that survival responses to climate

384 were the overwhelming driver of temporal trends in λ (Fig. 5). Individual growth
385 made no contribution to these trends because it was unresponsive to climate (Fig.
386 D,E,F), whereas flowering and fertility were responsive to climate but their role
387 was relatively small and imperceptible in Fig. 5. Furthermore, survival responses
388 to climate PC2 were the dominant driver of temporal trends, followed by PC3
389 and then PC1. Collectively, responses to PC2 and PC3 accounted for 91% of the
390 overall climate effect in back-casted values of λ .

391 Discussion

392 Understanding and predicting the effects of environmental change on plant demog-
393 raphy and population dynamics are urgent challenges. The integration of long-term
394 data with environmentally explicit demographic models provides a powerful vehicle
395 for meeting these challenges and may aid in identifying processes that drive some
396 populations into decline. By reconstructing 117 years of climate-dependent demog-
397 raphy, we tested the hypothesis that the extinction debt of our study population
398 was a consequence of recent climate change. Our results suggest the opposite: *C.*
399 *imbricata* is likely a climate change “winner”, on an accelerating trajectory toward
400 replacement-level within 38 years if current climate change trends persist, and
401 sooner if they accelerate. We further show that the strongest feature of climate
402 change in this system was not the main driver of population responses. Instead,
403 temporal trends in population viability were dominated by more subtle climatic
404 factors with relatively weak signals of recent change. Below, we interpret these
405 results in greater detail and discuss their broader significance.

406 Until recently, few plant demographic studies explicitly considered climatic

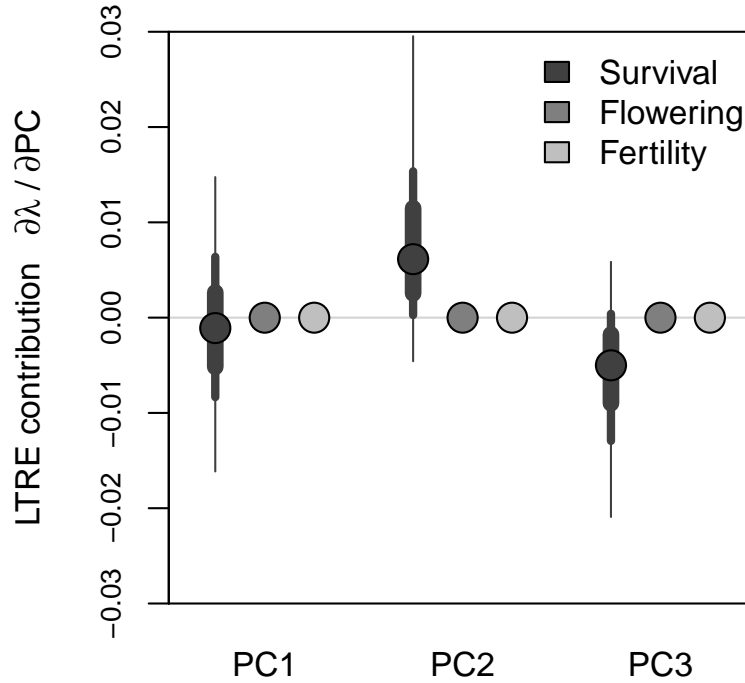


Figure 5: LTR decomposition of climate-driven inter-annual variability in population growth rates. Lines of decreasing thickness show the 50, 75 and 95 percentiles of the posterior distributions of the vital rate parameters, and points show the median. Shading corresponds to different vital rates (survival, flowering, and fertility) Posterior distributions for flowering and fertility are imperceptible on this scale.

407 drivers of inter-annual variation (Ehrlén *et al.*, 2016; Crone *et al.*, 2011), though
 408 this is rapidly changing. We are aware of no previous studies that have compared
 409 the magnitudes of different aspects of climate change alongside the magnitudes of
 410 demographic responses to those changes. However, we suspect that our key finding

411 – that the strongest dimension of climate change was not the strongest driver of
412 demography – may be common, since at the heart of this result lies the difference
413 between annual climate trends (captured by PC1) versus seasonal trends (PCs 2
414 and 3). Annual rainfall totals in our region have been decreasing but more of the
415 annual rainfall has been falling in the cool season, consistent with previous climata-
416 logical studies that suggest a shift from warm- to cool-season precipitation (Cook &
417 Seager, 2013; Cook *et al.*, 2015; Petrie *et al.*, 2014). Similarly, annual temperatures
418 have been increasing in our study region but it was cool-season warming, specif-
419 ically, that was most important for *C. imbricata* demography. Many plant and
420 animal life histories operate on seasonal schedules and may therefore be more sen-
421 sitive to seasonal redistribution of rainfall and temperature than to climate effects
422 that manifest over an entire year. Our results are consistent with previous studies
423 that demonstrate the importance of considering seasonal, not annual, drivers of
424 plant demographic responses (Selwood *et al.*, 2015; Williams *et al.*, 2015; Dahlgren
425 *et al.*, 2016). Some recent studies have taken a finer-grained approach, connecting
426 plant responses to weather events on monthly, weekly, or even daily time scales
427 (Teller *et al.*, 2016; Tenhumberg *et al.*, 2018; Shriver, 2016). For tractability, we
428 did not explore lagged climate effects beyond one year, though methods for doing
429 so are rapidly developing (Teller *et al.*, 2016; Tenhumberg *et al.*, 2018; Ogle *et al.*,
430 2015). Finding the appropriate timing and resolution of climate covariates is an
431 important area for future work in this system and more generally.

432 Rigorously accounting for various types of uncertainty is another an important
433 area in the development of environmentally explicit models for forecasting or back-
434 casting. Even with strong climate-demography relationships detected with our
435 unusually long-term data set, climate drivers accounted for little over half of the

inter-annual variation in λ during the study years. It was therefore important to place our predictions for historical growth rates in the context of the substantial uncertainty that arose from process error: all the additional, unspecified ways that years may differ. We have emphasized the positive trajectory of population viability as the most likely trend in λ , but this should be interpreted in light of the probability distributions that we provide (Fig. 4) – that is, with nuance and appropriate caution¹. As ecologists are increasingly called upon to forecast responses to change in climate drivers, it will be essential to do so in a probabilistic framework that accommodates process error, i.e., the variability *not* explained by climate drivers. Defining the temporal or spatial auto-correlation structure of process error (which we did not attempt) may further improve forecasts or backcasts.

Different aspects of a species' life cycle may respond in diverse ways to environmental drivers (Doak & Morris, 2010; Villellas *et al.*, 2015), highlighting the additional importance of considering multiple vital rates for understanding responses to global change. Our work was able to pinpoint which responses throughout the life cycle were most important for the overall population response to climate. Our results are consistent with previous findings that high-sensitivity vital rates (those that strongly influence λ , in this case survival and growth) are buffered against environmental variability while low-sensitivity vital rates (flowering and fertility) may exhibit wide fluctuations (Pfister, 1998). However, incomplete buffering of survival led to greater mortality in years with cold and dry cool-seasons – years that are becoming less frequent under climate change (Fig. 1) – and these survival responses

¹The probability that λ is increasing (0.714) matches the probability of a Clinton victory in the 2016 U.S. presidential election: <https://projects.fivethirtyeight.com/2016-election-forecast/>

dominated the overall increase in population viability over the past 120 years (Fig. 5). These results mirror a recent study of another long-lived perennial plant, the alpine sunflower *Helianthella quinquinervis*, where reproductive responses to climate drivers were strong but ultimately overwhelmed by weaker responses in survival that more strongly affected population growth (Iler *et al.*, 2019). It is commonly observed that demographic transitions related to growth and survival are the most important determinants of population viability in species with long-lived perennial life histories (Franco & Silvertown, 2004). It may therefore be a general result that climate effects on growth and survival will be more consequential in long-lived perennials than effects on reproductive processes, even as the latter exhibit greater sensitivity to climate, since perennials have many reproductive opportunities over potentially long lifespans (Dalglish *et al.*, 2010; Morris *et al.*, 2008).

Our historical reconstruction of climate-dependent population growth indicated that the climate has likely never been better for *C. imbricata* than it is now. This result begs the question of how these plants have reached their current, relatively high abundance, given over a century of population growth rates that were inferred to fall well below replacement levels. Land use history – which is not incorporated into our back-casted estimates – may have played a role. The Sevilleta NWR was exposed to grazing for much of the 20th century until 1973. Previous work suggests that cacti, and *C. imbricata* in particular, can increase in abundance in response to grazing, due to livestock dispersing detached stem segment and thus promoting asexual regeneration (Allen *et al.*, 1991). During our study, we observed recruitment to be almost exclusively from seed (sexual and asexual recruits are easily distinguishable), though it is possible that regeneration dynamics

484 were different under historical grazing regimes. Grazing may have also promoted
 485 cactus populations through release of competitive interactions with grasses (Yu
 486 *et al.*, 2019). Thus, one hypothesis is that *C. imbricata* achieved current densities
 487 under the historical land use regime, and cannot maintain these densities in the
 488 absence of cattle grazing. For long-lived plants, it may take decades to centuries
 489 for full payment of extinction debt driven by land use changes (Lehtilä *et al.*,
 490 2016; González-Varo *et al.*, 2015). An alternative hypothesis is that, independent
 491 of grazing or other land use history, our study population may be located in sink
 492 habitat and maintained by dispersal from nearby populations that are more viable.
 493 Indeed, previous work showed that *C. imbricata* at lower (by ca. 100 m) elevations
 494 had positive population growth rates (Miller *et al.*, 2009) and may therefore act
 495 as source populations. Regardless of which process or processes best account for
 496 the persistence of a population that is currently inviable, our results indicate that
 497 it will more likely than not be ‘rescued’ by ongoing climate change. One caveat
 498 to this conclusion is that, beyond the mean climate trends we have described, fu-
 499 ture climate (and especially monsoon precipitation) in our region is expected to
 500 be more variable (Rudgers *et al.*, 2018; Cook *et al.*, 2015) and this may dampen
 501 population growth independently of mean conditions (Boyce *et al.*, 2006). How-
 502 ever, our stochastic demographic analysis, which accounts for increasing climate
 503 variability during the 20th century, also showed a positive trajectory of λ_S (Fig.
 504 C4).

505 Previous studies of cacti have emphasized their sensitivity to freezing as a con-
 506 straint on physiological performance and geographic distribution (Flores & Yeaton,
 507 2003; Kinraide, 1978; Nobel, 1984). In our study, we detected an important role
 508 for winter minimum temperature and observed high mortality following record low

509 winter temperatures over a multi-day deep-freeze in 2011 (this is the low outlier
 510 in Fig. 4A). As these freezing events become less frequent under climate change,
 511 we expect an increase in regional abundance and perhaps northern expansion of
 512 *C. imbricata*'s range, which currently extends to southern Colorado and is likely
 513 limited by winter minimum temperatures. This may be an issue of applied concern
 514 in the region since *C. imbricata* is considered undesirable **due to its unpalatabil-**
 515 **ity to livestock** (Allen *et al.*, 1991). The role of cool-season precipitation that we
 516 detected was more surprising. A majority of annual precipitation in the South-
 517 west US comes from warm-season monsoon events (Adams & Comrie, 1997) and
 518 these events play a critical role in vegetation dynamics (Notaro & Gutzler, 2012;
 519 Petrie *et al.*, 2014), especially for plants with C4 and CAM photosynthesis that
 520 are physiologically most active during the warm summer months. Previous cactus
 521 demographic studies have emphasized the role of summer monsoon precipitation
 522 (Winkler *et al.*, 2018; Bowers, 2005). Our results suggest that, despite its summer-
 523 adapted CAM photosynthetic pathway, *C. imbricata* is able to capitalize on cool-
 524 season moisture, and this was an important component of the positive demographic
 525 effects of recent climate change. Similarly, Salguero-Gomez *et al.* (2012) identified
 526 *Cryptantha flava* as **a species likely to benefit from climate change** due in part to
 527 seasonal redistribution of rainfall that will lengthen its growing season.

528 Several limitations of our study warrant consideration in the interpretation of
 529 our results. First, our consideration of climate dependence was limited to four
 530 vital rate processes of established plants. Because we could not reliably assign a
 531 birth year to new recruits, we did not incorporate climate dependence in seedling
 532 recruitment. Previous studies of cactus demography suggest that seedling recruit-
 533 ment may be highly sensitive to climate, especially monsoon precipitation (e.g.,

534 Bowers 2005; Winkler *et al.* 2018). We suspect this is the case for *C. imbricata*,
535 since germination usually coincides with late-summer rains (*T.E.X. Miller, un-*
536 *publ. data*). Because we did not model this process as climate-dependent, our
537 results for climate effects on population growth are conservative. However, con-
538 sistent with expectations for long-lived perennials, we know seedling recruitment
539 to have very low eigenvalue sensitivities (Elder & Miller, 2016), which suggests
540 that even large climate effects on this process may not strongly register in terms
541 of population growth, as we observed for the reproductive functions of established
542 plants (Fig. 4B).

543 A second limitation is that our approach to quantifying climate drivers know-
544 ingly forfeits some information, and in two ways. First, in order to gain deep
545 temporal coverage, we relied on downscaled climate projections rather than direct
546 climatological observations. While these two types of data were correlated, they
547 were not perfectly so (Appendix A); this was especially true for temperature min-
548 ima and maxima (Table A1), where downscaled data likely mis-estimate localized
549 extremes. It is noteworthy that the downscaled climate data poorly captured the
550 extreme deep-freeze of winter 2011 (Fig. A1A). Poor demographic performance
551 in this year was consequently attributed to a statistical random effect (Fig. 4A),
552 though this was almost certainly a true climate effect. Second, we limited our
553 consideration of climate drivers to the first three principal components of inter-
554 annual variation. While these three components explained a large majority of the
555 variation (Fig. 1A), we are disregarding some of the more subtle dimensions of
556 climate variability and change. Given our main finding that the strongest features
557 of climate change are not the main determinants of population responses, these ne-
558 glected dimensions may include important demographic drivers. These two factors

mean that our conclusions for climate-dependence err on the conservative side.

To conclude, this study illustrates how long-term patterns of population viability can be reconstructed through climate-demography relationships observed on relatively short time scales. This allowed us to evaluate the hypothesis that recent climate change has driven *C. imbricata* in our region into extinction debt, a hypothesis that our data fail to support. Instead, this species is most likely benefitting from climate change, largely due to its positive responses, especially in survival, to recent and ongoing shifts in cool-season temperature and precipitation. Interestingly, changes in cool-season climate were not the strongest features of climate change, but they were nonetheless the most important determinants of population responses. The more general lesson for global change biologists is that relatively subtle dimensions of climate change may trigger strong ecological responses.

Acknowledgements

This study was supported by the Sevilleta LTER (NSF LTER awards 1440478, 1655499, and 1748133) and by NSF Division of Environmental Biology awards 1543651 and 1754468. We thank the Sevilleta National Wildlife Refuge staff (especially J. Erz) for facilitating research access. We thank M. Evans and E. Schultz for helpful discussions on modeling climate-demography relationships. Finally, we thank the many students and colleagues have contributed to this long-term study, especially M. Donald, A. Compagnoni, and B. Ochocki.

Author contributions

TEXM initiated and maintains the long-term study. KC collected and analyzed data and prepared a manuscript draft. TEXM finalized text and analyses. Both coauthors approve this submission.

Data accessibility

All of the code for our statistical and demographic modeling is available at https://github.com/texmiller/cholla_climate_IPM and raw data will be published in parallel with this manuscript.

References

- Ådahl E, Lundberg P, Jonzen N (2006) From climate change to population change: the need to consider annual life cycles. *Global Change Biology*, **12**, 1627–1633.
- Adams DK, Comrie AC (1997) The north american monsoon. *Bulletin of the American Meteorological Society*, **78**, 2197–2214.
- Adler PB, Byrne KM, Leiker J (2013) Can the past predict the future? experimental tests of historically based population models. *Global change biology*, **19**, 1793–1803.
- Allen L, Allen E, Kunst C, Sosebee R (1991) A diffusion model for dispersal of *Opuntia imbricata* (cholla) on rangeland. *The Journal of Ecology*, pp. 1123–1135.

- 598 Bowers JE (2005) Influence of climatic variability on local population dynamics of
599 a sonoran desert platyopuntia. *Journal of Arid Environments*, **61**, 193–210.
- 600 Boyce MS, Haridas CV, Lee CT, Group NSDW, *et al.* (2006) Demography in an
601 increasingly variable world. *Trends in Ecology & Evolution*, **21**, 141–148.
- 602 Buckley LB, Kingsolver JG (2012) The demographic impacts of shifts in climate
603 means and extremes on alpine butterflies. *Functional Ecology*, **26**, 969–977.
- 604 Caswell H (2001) *Matrix Population Models*. Sinauer Associates, Inc., Sunderland,
605 MA, 2 edn.
- 606 Compagnoni A, Bibian AJ, Ochocki BM, *et al.* (2016) The effect of demographic
607 correlations on the stochastic population dynamics of perennial plants. *Ecolog-
608 ical Monographs*, **86**, 480–494.
- 609 Cook B, Seager R (2013) The response of the north american monsoon to increased
610 greenhouse gas forcing. *Journal of Geophysical Research: Atmospheres*, **118**,
611 1690–1699.
- 612 Cook BI, Ault TR, Smerdon JE (2015) Unprecedented 21st century drought risk
613 in the american southwest and central plains. *Science Advances*, **1**, e1400082.
- 614 Crone EE, Menges ES, Ellis MM, *et al.* (2011) How do plant ecologists use matrix
615 population models? *Ecology letters*, **14**, 1–8.
- 616 Dahlgren JP, Bengtsson K, Ehrlén J (2016) The demography of climate-driven and
617 density-regulated population dynamics in a perennial plant. *Ecology*.

- 618 Dalglish HJ, Koons DN, Adler PB (2010) Can life-history traits predict the re-
619 sponse of forb populations to changes in climate variability? *Journal of Ecology*,
620 **98**, 209–217.
- 621 Dalglish HJ, Koons DN, Hooten MB, Moffet CA, Adler PB (2011) Climate influ-
622 ences the demography of three dominant sagebrush steppe plants. *Ecology*, **92**,
623 75–85.
- 624 Daly C, Halbleib M, Smith JI, *et al.* (2008) Physiographically sensitive mapping
625 of climatological temperature and precipitation across the conterminous united
626 states. *International Journal of Climatology: a Journal of the Royal Meteorolo-*
627 *gical Society*, **28**, 2031–2064.
- 628 Dinno A (2018) *paran: Horn's Test of Principal Components/Factors*. URL [https:](https://CRAN.R-project.org/package=paran)
629 [//CRAN.R-project.org/package=paran](https://CRAN.R-project.org/package=paran). R package version 1.5.2.
- 630 Doak DF, Morris WF (2010) Demographic compensation and tipping points in
631 climate-induced range shifts. *Nature*, **467**, 959.
- 632 Dullinger S, Gatttringer A, Thuiller W, *et al.* (2012) Extinction debt of high-
633 mountain plants under twenty-first-century climate change. *Nature Climate*
634 *Change*, **2**, 619.
- 635 Dybala KE, Eadie JM, Gardali T, Seavy NE, Herzog MP (2013) Projecting de-
636 mographic responses to climate change: adult and juvenile survival respond
637 differently to direct and indirect effects of weather in a passerine population.
638 *Global Change Biology*, **19**, 2688–2697.

- 639 Ehrlén J, Morris WF (2015) Predicting changes in the distribution and abundance
640 of species under environmental change. *Ecology Letters*, **18**, 303–314.
- 641 Ehrlén J, Morris WF, von Euler T, Dahlgren JP (2016) Advancing environmentally
642 explicit structured population models of plants. *Journal of Ecology*, **104**, 292–
643 305.
- 644 Elderd BD, Miller TE (2016) Quantifying demographic uncertainty: Bayesian
645 methods for integral projection models. *Ecological Monographs*, **86**, 125–144.
- 646 Flores JL, Yeaton R (2003) The replacement of arborescent cactus species along a
647 climatic gradient in the southern chihuahuan desert: competitive hierarchies and
648 response to freezing temperatures. *Journal of arid environments*, **55**, 583–594.
- 649 Franco M, Silvertown J (2004) A comparative demography of plants based upon
650 elasticities of vital rates. *Ecology*, **85**, 531–538.
- 651 Franklin SB, Gibson DJ, Robertson PA, Pohlmann JT, Fralish JS (1995) Parallel
652 analysis: a method for determining significant principal components. *Journal of*
653 *Vegetation Science*, **6**, 99–106.
- 654 Frederiksen M, Daunt F, Harris MP, Wanless S (2008) The demographic impact
655 of extreme events: stochastic weather drives survival and population dynamics
656 in a long-lived seabird. *Journal of Animal Ecology*, **77**, 1020–1029.
- 657 George EI, McCulloch RE (1993) Variable selection via gibbs sampling. *Journal*
658 *of the American Statistical Association*, **88**, 881–889.
- 659 González-Varo JP, Albaladejo RG, Aizen MA, Arroyo J, Aparicio A (2015) Ex-

660 tinction debt of a common shrub in a fragmented landscape. *Journal of Applied*
661 *Ecology*, **52**, 580–589.

662 Hastings A, Abbott KC, Cuddington K, *et al.* (2018) Transient phenomena in
663 ecology. *Science*, **361**, eaat6412.

664 Hijmans RJ, Cameron SE, Parra JL, Jones PG, Jarvis A (2005) Very high reso-
665 lution interpolated climate surfaces for global land areas. *International Journal*
666 *of Climatology: A Journal of the Royal Meteorological Society*, **25**, 1965–1978.

667 Hooten MB, Hobbs N (2015) A guide to bayesian model selection for ecologists.
668 *Ecological Monographs*, **85**, 3–28.

669 Hylander K, Ehrlén J (2013) The mechanisms causing extinction debts. *Trends in*
670 *ecology & evolution*, **28**, 341–346.

671 Iler AM, Compagnoni A, Inouye DW, Williams JL, CaraDonna PJ, Anderson
672 A, Miller TE (2019) Reproductive losses due to climate change-induced earlier
673 flowering are not the primary threat to plant population viability in a perennial
674 herb. *Journal of Ecology*, **107**, 1931–1943.

675 Jenouvrier S, Caswell H, Barbraud C, Holland M, Strøve J, Weimerskirch H (2009)
676 Demographic models and ipcc climate projections predict the decline of an em-
677 peror penguin population. *Proceedings of the National Academy of Sciences*,
678 **106**, 1844–1847.

679 Jenouvrier S, Holland M, Stroeve J, Serreze M, Barbraud C, Weimerskirch H,
680 Caswell H (2014) Projected continent-wide declines of the emperor penguin un-
681 der climate change. *Nature Climate Change*, **4**, 715.

- 682 Kinraide TB (1978) The ecological distribution of cholla cactus (*Opuntia imbricata*
683 (haw.) dc.) in el paso county, colorado. *The Southwestern Naturalist*, pp. 117–
684 133.
- 685 Kuussaari M, Bommarco R, Heikkinen RK, *et al.* (2009) Extinction debt: a chal-
686 lenge for biodiversity conservation. *Trends in ecology & evolution*, **24**, 564–571.
- 687 Lehtilä K, Dahlgren JP, Garcia MB, Leimu R, Syrjänen K, Ehrlén J (2016) For-
688 est succession and population viability of grassland plants: long repayment of
689 extinction debt in *Primula veris*. *Oecologia*, **181**, 125–135.
- 690 Lynch HJ, Rhainds M, Calabrese JM, Cantrell S, Cosner C, Fagan WF (2014) How
691 climate extremes—not means—define a species’ geographic range boundary via
692 a demographic tipping point. *Ecological Monographs*, **84**, 131–149.
- 693 Maschinski J, Baggs JE, QUINTANA-ASCENCIO PF, Menges ES (2006) Using
694 population viability analysis to predict the effects of climate change on the ex-
695 tinction risk of an endangered limestone endemic shrub, arizona cliffrose. *Con-*
696 *servation Biology*, **20**, 218–228.
- 697 McLean N, Lawson CR, Leech DI, van de Pol M (2016) Predicting when climate-
698 driven phenotypic change affects population dynamics. *Ecology Letters*, **19**,
699 595–608.
- 700 Miller TE, Louda SM, Rose KA, Eckberg JO (2009) Impacts of insect herbivory on
701 cactus population dynamics: experimental demography across an environmental
702 gradient. *Ecological Monographs*, **79**, 155–172.

- 703 Morris WF, Pfister CA, Tuljapurkar S, *et al.* (2008) Longevity can buffer plant and
704 animal populations against changing climatic variability. *Ecology*, **89**, 19–25.
- 705 Morrison SF, Hik DS (2007) Demographic analysis of a declining pika ochotona
706 collaris population: linking survival to broad-scale climate patterns via spring
707 snowmelt patterns. *Journal of Animal ecology*, **76**, 899–907.
- 708 Nobel PS (1984) Extreme temperatures and thermal tolerances for seedlings of
709 desert succulents. *Oecologia*, **62**, 310–317.
- 710 Notaro M, Gutzler D (2012) Simulated impact of vegetation on climate across the
711 north american monsoon region in ccs3. 5. *Climate dynamics*, **38**, 795–814.
- 712 Ogle K, Barber JJ, Barron-Gafford GA, *et al.* (2015) Quantifying ecological mem-
713 ory in plant and ecosystem processes. *Ecology letters*, **18**, 221–235.
- 714 Ohm JR, Miller TE (2014) Balancing anti-herbivore benefits and anti-pollinator
715 costs of defensive mutualists. *Ecology*, **95**, 2924–2935.
- 716 Peters DP, Havstad KM, Archer SR, Sala OE (2015) Beyond desertification: new
717 paradigms for dryland landscapes. *Frontiers in Ecology and the Environment*,
718 **13**, 4–12.
- 719 Petrie M, Collins S, Gutzler D, Moore D (2014) Regional trends and local variabil-
720 ity in monsoon precipitation in the northern chihuahuan desert, usa. *Journal of*
721 *arid environments*, **103**, 63–70.
- 722 Pfister CA (1998) Patterns of variance in stage-structured populations: evolution-
723 ary predictions and ecological implications. *Proceedings of the National Academy*
724 *of Sciences*, **95**, 213–218.

- 725 Plummer M, *et al.* (2003) Jags: A program for analysis of bayesian graphical
726 models using gibbs sampling. In: *Proceedings of the 3rd international workshop*
727 *on distributed statistical computing*, vol. 124. Vienna, Austria.
- 728 Rudgers JA, Chung YA, Maurer GE, Moore DI, Muldavin EH, Litvak ME, Collins
729 SL (2018) Climate sensitivity functions and net primary production: A frame-
730 work for incorporating climate mean and variability. *Ecology*, **99**, 576–582.
- 731 Salguero-Gomez R, Siewert W, Casper BB, Tielbörger K (2012) A demographic
732 approach to study effects of climate change in desert plants. *Philosophical Trans-*
733 *actions of the Royal Society B: Biological Sciences*, **367**, 3100–3114.
- 734 Selwood KE, McGeoch MA, Mac Nally R (2015) The effects of climate change
735 and land-use change on demographic rates and population viability. *Biological*
736 *Reviews*, **90**, 837–853.
- 737 Shriver RK (2016) Quantifying how short-term environmental variation leads to
738 long-term demographic responses to climate change. *Journal of Ecology*, **104**,
739 65–78.
- 740 Sletvold N, Dahlgren JP, Øien DI, Moen A, Ehrlén J (2013) Climate warming alters
741 effects of management on population viability of threatened species: results from
742 a 30-year experimental study on a rare orchid. *Global Change Biology*, **19**, 2729–
743 2738.
- 744 Smith M, Caswell H, Mettler-Cherry P (2005) Stochastic flood and precipitation
745 regimes and the population dynamics of a threatened floodplain plant. *Ecological*
746 *Applications*, **15**, 1036–1052.

- 747 Su YS, Yajima M (2012) R2jags: A package for running jags from r. *R package*
748 *version 0.03-08*, URL <http://CRAN.R-project.org/package=R2jags>.
- 749 Teller BJ, Adler PB, Edwards CB, Hooker G, Ellner SP (2016) Linking demogra-
750 phy with drivers: climate and competition. *Methods in Ecology and Evolution*,
751 **7**, 171–183.
- 752 Tenhumberg B, Crone EE, Ramula S, Tyre AJ (2018) Time-lagged effects of
753 weather on plant demography: drought and astragalus scaphoides. *Ecology*,
754 **99**, 915–925.
- 755 Urban MC (2015) Accelerating extinction risk from climate change. *Science*, **348**,
756 571–573.
- 757 Van de Pol M, Vindenes Y, Sæther BE, Engen S, Ens BJ, Oosterbeek K, Tinbergen
758 JM (2010) Effects of climate change and variability on population dynamics in
759 a long-lived shorebird. *Ecology*, **91**, 1192–1204.
- 760 Vellend M, Verheyen K, Jacquemyn H, Kolb A, Van Calster H, Peterken G, Hermy
761 M (2006) Extinction debt of forest plants persists for more than a century fol-
762 lowing habitat fragmentation. *Ecology*, **87**, 542–548.
- 763 Villellas J, Doak DF, García MB, Morris WF (2015) Demographic compensation
764 among populations: what is it, how does it arise and what are its implications?
765 *Ecology letters*, **18**, 1139–1152.
- 766 Wang T, Hamann A, Spittlehouse D, Carroll C (2016) Locally downscaled and
767 spatially customizable climate data for historical and future periods for north
768 america. *PLoS One*, **11**, e0156720.

- 769 Williams JL, Jacquemyn H, Ochocki BM, Brys R, Miller TE (2015) Life history
770 evolution under climate change and its influence on the population dynamics of
771 a long-lived plant. *Journal of Ecology*, **103**, 798–808.
- 772 Williams JL, Miller TEX, Ellner SP (2012) Avoiding unintentional eviction from
773 integral projection models. *Ecology*, **93**, 2008–2014.
- 774 Winkler DE, Conner JL, Huxman TE, Swann DE (2018) The interaction of drought
775 and habitat explain space–time patterns of establishment in saguaro (*Carnegiea*
776 *gigantea*). *Ecology*, **99**, 621–631.
- 777 Yu K, D’Odorico P, Collins SL, *et al.* (2019) The competitive advantage of a con-
778 stitutive CAM species over a C4 grass species under drought and CO2 enrichment.
779 *Ecosphere*, **10**, e02721.

780 Appendix A: Correspondence between downscaled 781 and locally measured climate variables

782 Correlation of climate values

783 We compared warm- and cool-season values of four climate variables (total pre-
784 cipitation and minimum, mean, and maximum temperature) between two data
785 sources: the SEV-LTER meteorological station nearest our study site (station 50 in
786 the SEV-LTER meteorological network) and downscaled data from ClimateWNA
787 corresponding to the same latitude, longitude, and elevation as station 50. Our
788 goal was to determine how well the downscaled data captured conditions ‘on the
789 ground’ as measured directly by the meteorological station. We compared the
790 years 2001 through 2017, which are the years of overlap between the two data
791 sources.

792 There was moderate to strong agreement between the two data sources (Table
793 A1, Fig. A1, Fig. A2). Temperature extrema were less strongly correlated between
794 the two data sets than temperature means (Fig. A1), which is unsurprising given
795 that extreme values may be sensitive to local micro-environmental conditions that
796 the relatively coarse downscaled data would miss. There was an extreme-cold
797 event in 2010 that was particularly poorly captured by the downscaled data (Fig.
798 A1A). The weakest correlation was that of warm-season maximum temperature
799 (Fig. A1F; Pearson’s $r = 0.41$, $P = 0.11$).

Table A1: Correlations between seasonal climate values measured by an on-site meteorological station versus downscaled data from ClimateWNA corresponding to the same years and location. Correlation values show Pearson correlations and P-values come from t -tests with 14 degrees of freedom.

Season	Variable	Correlation	P-value
Warm	Min temperature	0.59	0.0153
Warm	Mean temperature	0.84	10^{-4}
Warm	Max temperature	0.41	0.1135
Warm	Precipitation	0.49	0.0544
Cool	Min temperature	0.51	0.0622
Cool	Mean temperature	0.94	3.6×10^{-7}
Cool	Max temperature	0.69	0.0069
Cool	Precipitation	0.87	4.6×10^{-5}

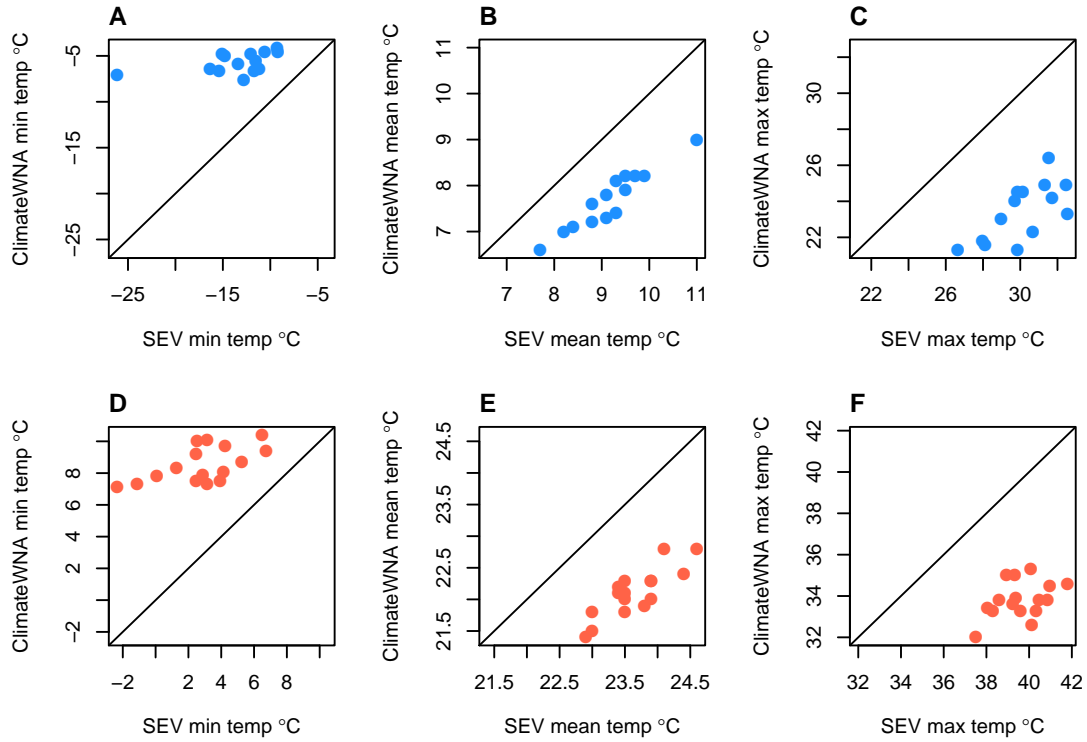


Figure A1: Correlations of minimum, mean, and maximum temperature values of cool (A–C) and warm (D–F) seasons between SEV-LTER meteorological data and downscaled estimates from ClimateWNA for years 2004–2017. Diagonal lines show $y = x$.

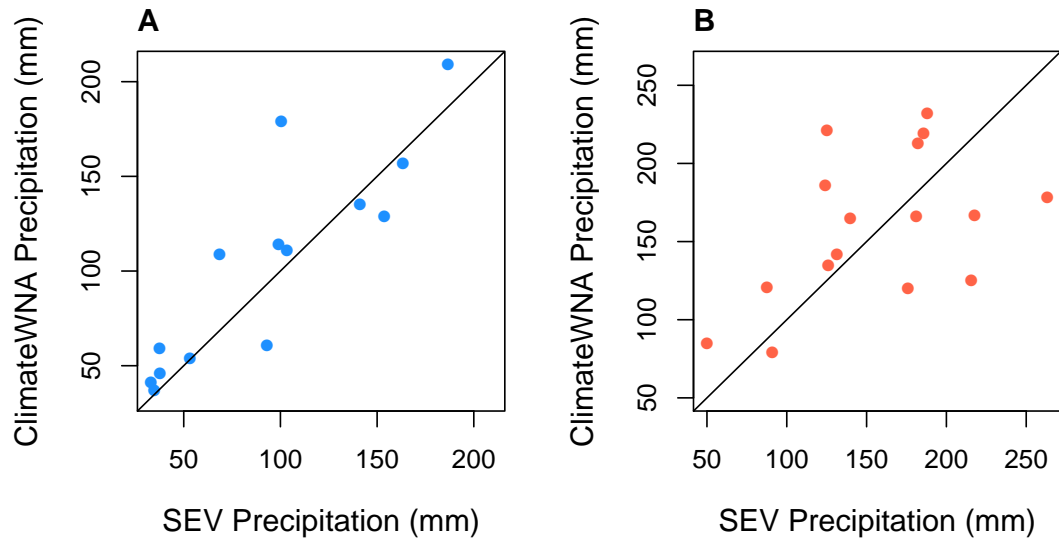


Figure A2: Correlations of cool- (**A**) and warm-season (**B**) precipitation between SEV-LTER meteorological data and downscaled estimates from ClimateWNA for years 2004–2017. Diagonal lines show $y = x$.

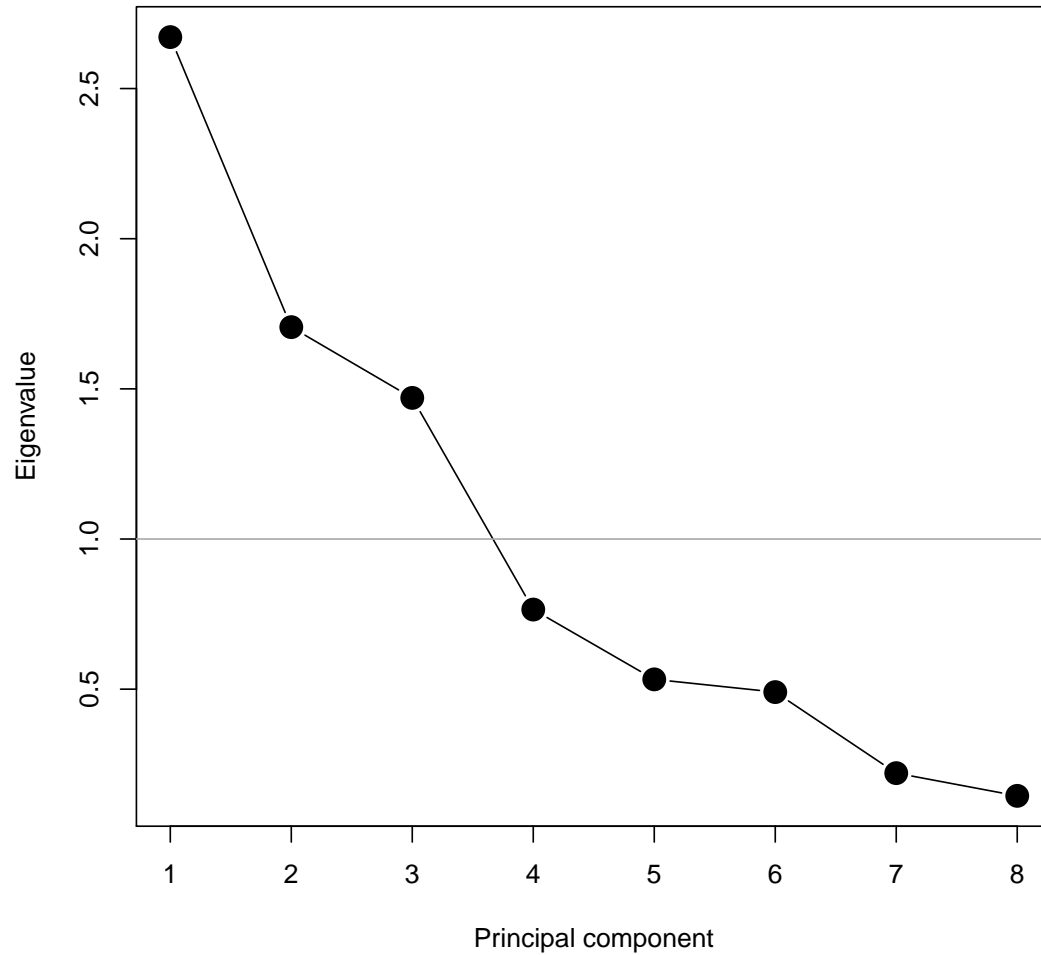


Figure A3: Results of parallel analysis conducted using the R package ‘paran’ (Dinno, 2018). Components with eigenvalues greater than 1 are retained.

800 Re-analysis with SEV-LTER data

801 To further explore the consequences of relying on down-scaled climate data, we
 802 re-ran our demographic analysis using the SEV-LTER meteorological data and

803 compared the results to those based on ClimateWNA. First, we conducted PCA on
804 raw seasonal temperature and precipitation values from SEV Meteorological Sta-
805 tion 50 over the observation years 2004–2017. As in our analysis of ClimateWNA
806 data, parallel analysis supported retention of three principal components. Vari-
807 able loadings onto these PCs are shown in Fig. A4 and show a pattern similar to
808 ClimateWNA data whereby PC1 was dominated by annual differences (cool- and
809 warm-season variables loaded similarly) and PC2-3 were dominated by seasonal
810 climate factors. Second, we fit the full set of vital rate models to these three PCs
811 and used stochastic variable selection (Appendix B) to eliminate weakly supported
812 climate covariates. We then re-fit the vital rate models including variables with
813 $\hat{z}_i > 0.1$ (see Appendix B). These fitted models are shown in Fig. A5.

814 We compared results based on the two data sources in several ways. First,
815 we compared the inter-annual variances associated with year random effects in
816 the statistical models. We found that, for survival in particular, random variance
817 across years was much lower using SEV-LTER data as climate covariates com-
818 pared to ClimateWNA (Fig. A6). This tells us that, as expected, on-site data
819 provided greater resolution of climate drivers, since less inter-annual variation in
820 survival was attributed to process error. Second, we used the IPM derived from
821 each data source to generate two predicted time series of λ during the study years.
822 We found that SEV-LTER climate PCs explained 78% of inter-annual variation
823 in λ , an improvement over the 60% explained by ClimateWNA PCs. Finally, the
824 year-by-year estimates were significantly correlated between the two data sources
825 (Fig. A7A; Pearson’s $r = 0.59$, $t_{10} = 2.34$, $P < 0.04$). When we additionally incor-
826 porated year-specific random effects estimated from the statistical models, λ esti-
827 mates were nearly perfectly correlated (Fig. A7B; Pearson’s $r = 0.99$, $t_{10} = 40.36$,

828 $P < 0.0001$), as expected. This tells us that our qualitative conclusions based on
 829 the longer ClimateWNA time series of climate covariates is likely robust to the
 830 uncertainties introduced by downscaled data. However, the 18% loss of resolution
 831 with ClimateWNA tells us that using downscaled data inflated the contribution
 832 of process error to our back-casted estimates (Fig. C3A).

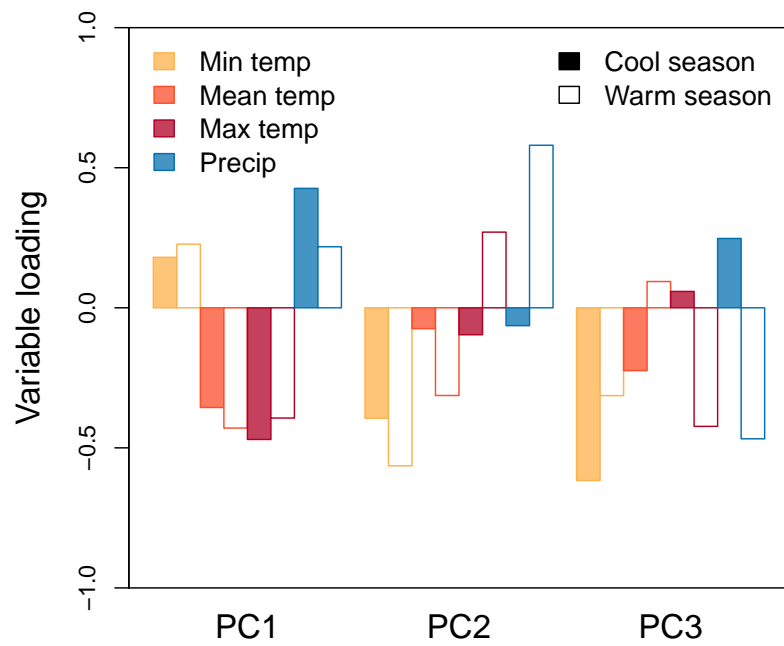


Figure A4: Principal components analysis of SEV-LTER meteorological data. Bars show loadings of raw variables onto three principal components. Layout as in Fig. 1.

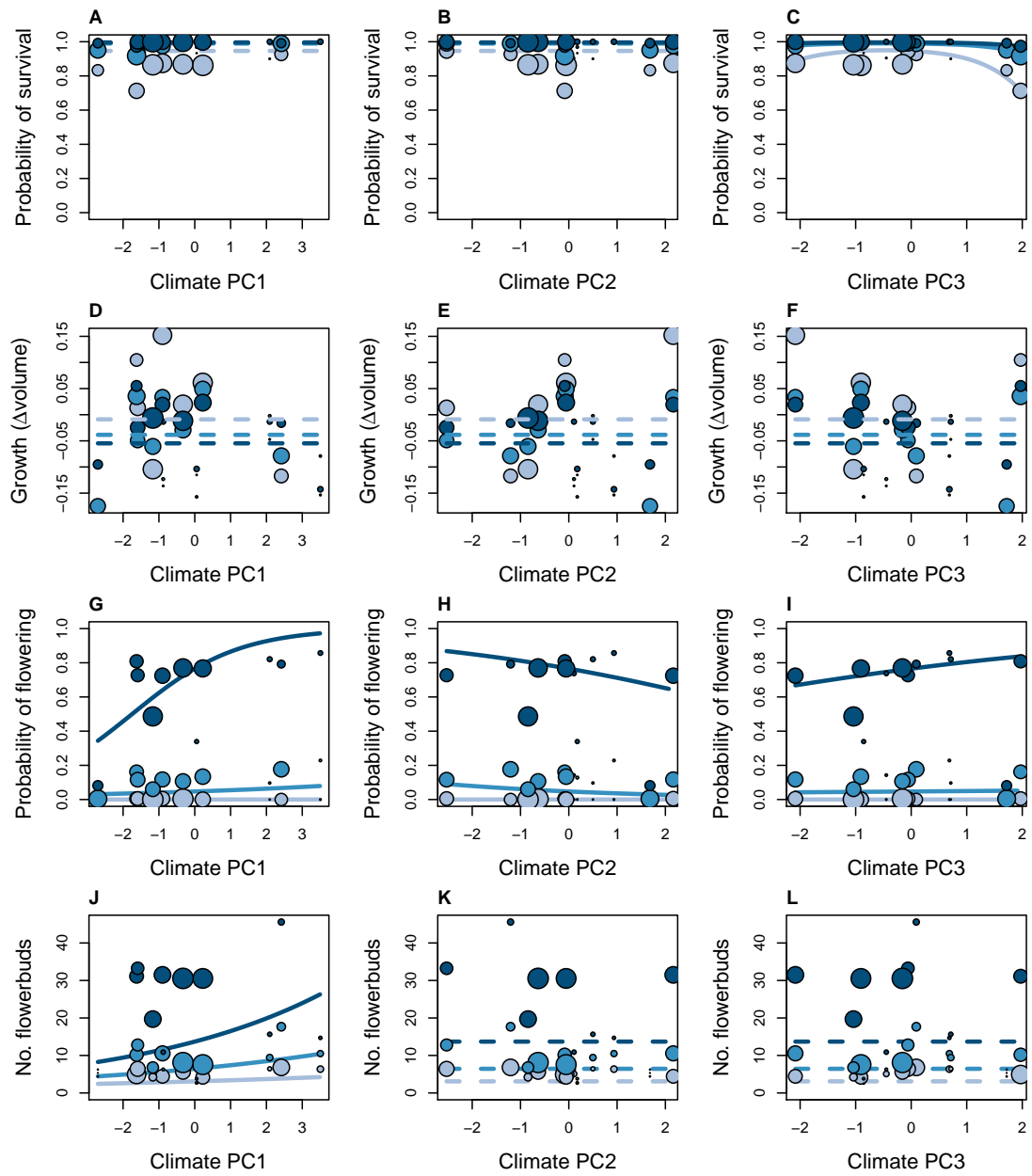


Figure A5: Vital rate data and fitted models using principal components of SEV-LTER meteorological data as climate covariates. Layout as in Fig. 2.

Climate PC	Model term	Survival	Growth	Flowering	Fertility
	Size	1	0.01	1	1
1	PC	0.06	0.01	0.07	0.07
1	PC*PC	0.03	0.01	0.05	0.01
1	PC*size	0.06	0.01	1	0.31
2	PC	0.06	0.01	0.13	0.05
2	PC*PC	0.03	0.01	0.05	0.03
2	PC*size	0.02	0.01	0.04	0.03
3	PC	0.78	0.02	0.09	0.04
3	PC*PC	0.88	0.02	0.08	0.03
3	PC*size	0.04	0.01	0.17	0.02

Table A2: Stochastic variable selection results based on climate data from SEV-LTER. Values (z) can be interpreted as the probability that a model coefficient is non-zero. Bolded values indicate terms retained in the final model.

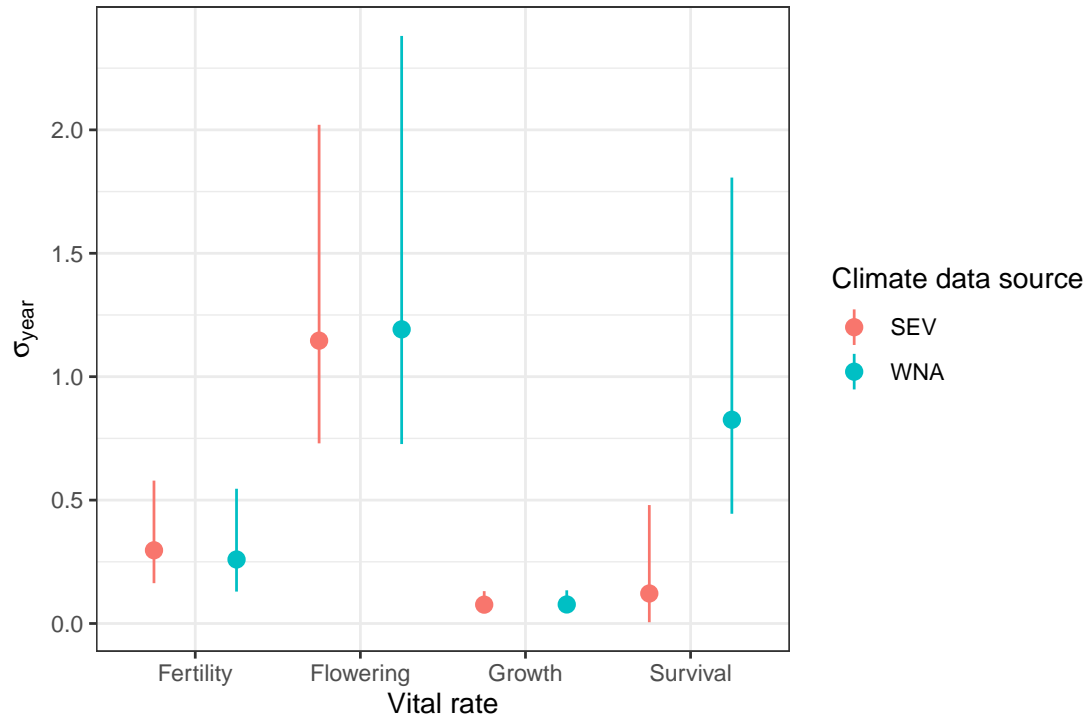


Figure A6: Posterior distributions of inter-annual variance (σ_{year}) associated with year random effects from vital rate models fit with two climate data sources (colors): ClimateWNA and SEV-LTER. Points show posterior means and bars show 95% credible intervals.

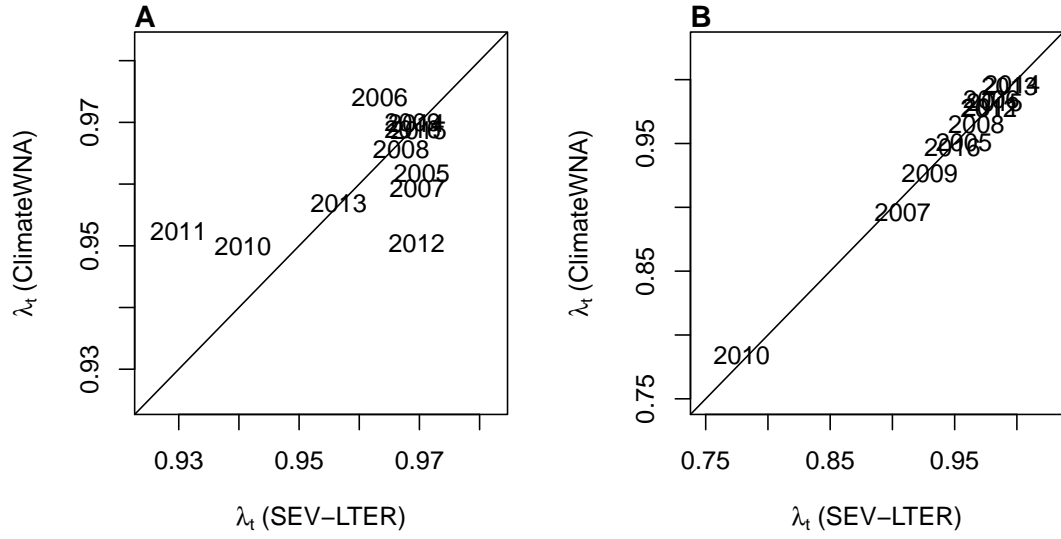


Figure A7: Comparison of year-specific estimates of λ from IPMs using either SEV-LTER (x -axis) or ClimateWNA (y -axis) as climate data sources. Diagonal lines show $y = x$. **A**, λ estimates based only on climate PCs (Pearson's $r = 0.59$, $t_{10} = 2.34$, $P < 0.04$); **B**, λ estimates based on climate and year random effects, which account for inter-annual differences not explained by the climate PCs (Pearson's $r = 0.99$, $t_{10} = 40.36$, $P < 0.0001$).

833 Appendix B: Stochastic variable selection

834 Because we intended to extrapolate the vital rate models into past climate environ-
835 ments that were not well represented during the long-term study, it was important
836 that we simplify the vital rate models to exclude unnecessary coefficients (which,
837 even if small in absolute value, could generate unrealistic predictions when ex-
838 trapolated over a greater range of climate than the models were fitted to). To
839 do this, we used stochastic variable selection, a ‘model-based model selection’
840 approach (Hooten & Hobbs, 2015) that generates weightings for each fixed-effect
841 coefficient, indicating the probability that the coefficient is non-zero. We employed
842 an approach based on George and McCulloch (1993) where each coefficient (C_i)
843 is modeled as a mixture distribution with zero and non-zero modes, where modal
844 frequency is determined by an indicator variable (z_i). The coefficient prior was:

$$C_i \sim (1 - z_i) * N(0, 0.1) + z_i * N(0, 1000) \quad (\text{B1})$$

$$z_i \sim \text{Bernoulli}(0.5) \quad (\text{B2})$$

845 The first term of the mixture distribution assigns, with probability $(1 - z_i)$, a
846 prior with mean zero and arbitrarily small variance, effectively forcing the poste-
847 rior estimate to equal zero. The second term assigns, with probability z_i , a prior
848 with mean zero and arbitrarily large variance, which allows for a non-zero pos-
849 terior estimate. The posterior distribution of the indicator variable z_i gives the
850 probability that the coefficient is non-zero. We estimated this probability for each
851 coefficient in Eq. B1 and retained in the final model all coefficients with a posterior

mean $\hat{z}_i > 0.1$, meaning that the model term is determined to be non-zero with
90% confidence. All z_i values from the full model are shown in Table B1.

Climate PC	Model term	Survival	Growth	Flowering	Fertility
	Size	1	0.53	1	1
1	PC	0.13	0.04	0.12	0.05
1	PC*PC	0.03	0.01	0.03	0.01
1	PC*size	0.06	0.01	0.08	0.07
2	PC	0.18	0.03	0.11	0.14
2	PC*PC	0.06	0.01	0.06	0.03
2	PC*size	0.04	0.02	1	0.27
3	PC	0.18	0.02	0.12	0.18
3	PC*PC	0.09	0.01	0.09	0.06
3	PC*size	0.06	0.01	0.13	0.03

Table B1: Stochastic variable selection results. Values (z) can be interpreted as the probability that a model coefficient is non-zero. Bolded values indicate terms retained in the final model.

854 Appendix C: Additional demographic modeling meth- 855 ods and results

856 We estimated a time series for the stochastic population growth rate (λ_S) over
857 the period 1900-2017 using a moving window approach. While the determinis-
858 tic growth rate for each year estimates the long-run growth rate expected if the
859 conditions of that year remained constant, the stochastic growth rate integrated
860 over a broader range of conditions, incorporating year-to-year fluctuations and
861 auto-correlation of climate variables.

We simulated population dynamics according to Equations 4–2 to estimate the stochastic population growth rate λ_S . We estimated λ_S for 10-year windows spanning the time series 1901–2017, such that the value of λ_S for year t reflects the stochastic growth rate for a climate environment defined by years t through $t + 9$. For each 10-year window, we simulated 1000 years of population dynamics, each year randomly drawing one of the 10 climate-years. For each year of the simulation, we calculated total population size as:

$$N_t = \int n(x)_t dx + B_{1,t} + B_{2,t} \quad (\text{C1})$$

and estimated the stochastic growth rate for that window as the expected value of the one-year growth rate:

$$\log(\lambda_S) = \mathbb{E}[\log(\frac{N_{t+1}}{N_t})] \quad (\text{C2})$$

Table C1: Parameter values of tree cholla IPM.

Parameter description	Symbol	Mean	95%CI
Survival coefficients	β_0	3.33	(1.4 – 5.25)
	β_1	1.31	(1.18 – 1.44)
	ρ_1^1	-0.11	(-0.82 – 0.61)
	ρ_1^2	0.41	(-0.25 – 1.13)
	ρ_1^3	-0.28	(-0.84 – 0.3)
Growth coefficients	β_0	-0.03	(-0.08 – 0.02)
	β_1	-0.02	(-0.03 – -0.02)
Growth standard deviation	σ	0.25	(0.25 – 0.26)
Flowering coefficients	β_0	-4.76	(-7.37 – -2.22)
	β_1	5.17	(4.78 – 5.54)
	ρ_1^1	-0.26	(-1.27 – 0.7)
	ρ_1^2	0.07	(-0.85 – 1.01)
	ρ_3^2	1.11	(0.65 – 1.61)
	ρ_1^3	-0.04	(-0.79 – 0.77)
	ρ_3^3	0.21	(-0.06 – 0.47)
Fertility coefficients	β_0	-0.25	(-0.6 – 0.1)
	β_1	2.22	(2.01 – 2.42)
	ρ_1^2	0.06	(-0.15 – 0.28)
	ρ_3^2	0.17	(-0.01 – 0.35)
	ρ_1^3	0.12	(-0.04 – 0.29)
Seeds per fruit	κ	113.46	(93.47 – 132.59)
Recruitment into seed bank	δ	0.03	(0.02 – 0.05)
Germination rates	γ_1	0.0059	(0.0047 – 0.0073)
	γ_2	0.0044	(0.0033 – 0.0056)
Seedling size distribution	μ_s	-3.49	(-3.62 – -3.37)
	σ_s	0.23	(0.15 – 0.35)
Seedling survival	ω	0.5	(0.002 – 0.998)
Size bounds	L	-3.94	
	U	1.89	

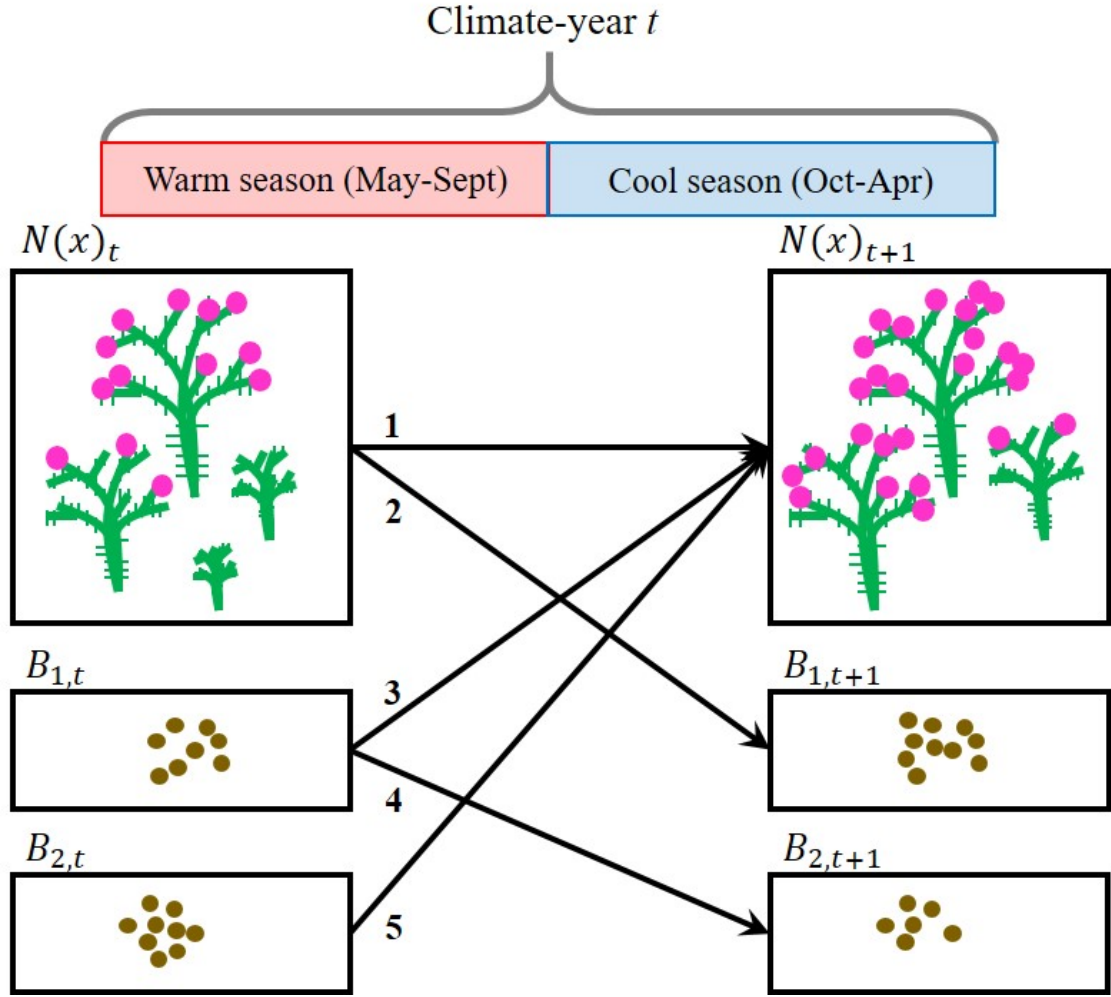


Figure C1: *C. imbricata* life cycle and census timing with respect to warm- and cool-season climate. Numbered arrows correspond to demographic events that occur during a transition year: (1) established plants survive and grow, (2) plants that are reproductive in year t contribute seeds that will make up the 1-yo seed bank in year $t+1$, (3) a fraction of seeds in the 1-yo seed bank survive and recruit into the plant population as seedlings in year $t+1$, (4) another fraction of seeds in the 1-yo seed bank survives and remains to form the 2-yo seed bank in year $t+1$, (5) a fraction of seeds in the 2-yo seed bank survive and recruit into the plant population as seedlings in year $t+1$. Survival and growth from year t to year $t+1$ (arrow 1) depended on climate year year t , whereas flowering and flowerbud production in year t (components of arrow 2) depended on climate in year $t-1$.

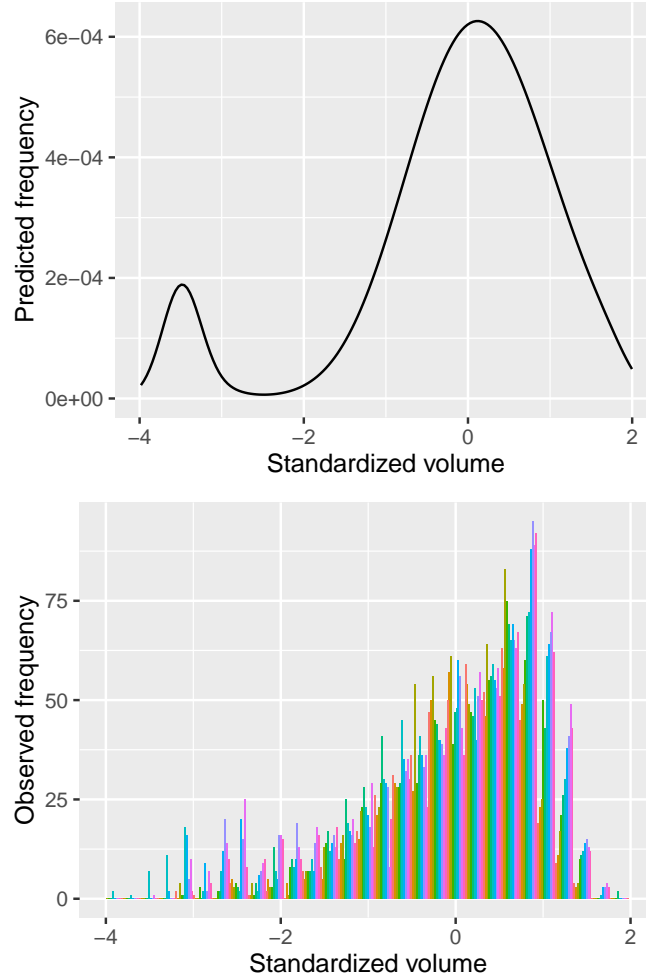


Figure C2: Comparison of predicted (top) and observed (bottom) size distributions, where size was the natural logarithm of plant volume standardized to mean zero. In the bottom panel, different colors represent different years. The predicted stable size distribution (evaluated at the average climate) corresponded well to the observed size distribution, though very large plants were over-represented in the observed distribution. This is consistent with the idea that the population may have recently transitioned into decline, whereby the persistence of large plants may reflect a legacy of positive growth rates. Also, the peak for new recruits was at a larger size in the observed distribution, but this was likely a consequence of the fact that we rarely detected new recruits. The “new” plants in our plots each year were likely several years old.

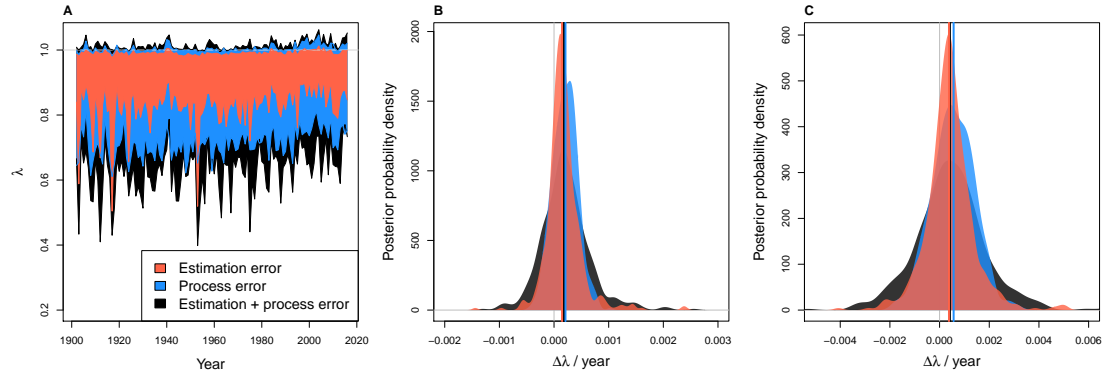


Figure C3: **A**, Time series of back-casted asymptotic population growth rates (λ) predicted based on inter-annual variation in three climate PCs. Shaded regions show the 95% credible interval of the posterior probability distributions for three uncertainty scenarios: estimation error only (parameter uncertainty; red), process error only (year-to-year heterogeneity unrelated to the climate PCs; blue), and both estimation and process error (black). **B**, **C**, Posterior probability distribution for the change in λ per year based on the entire time series (**B**) or years since 1970 (**C**). Vertical lines show the medians of the posterior distributions. Colors as in **A**.

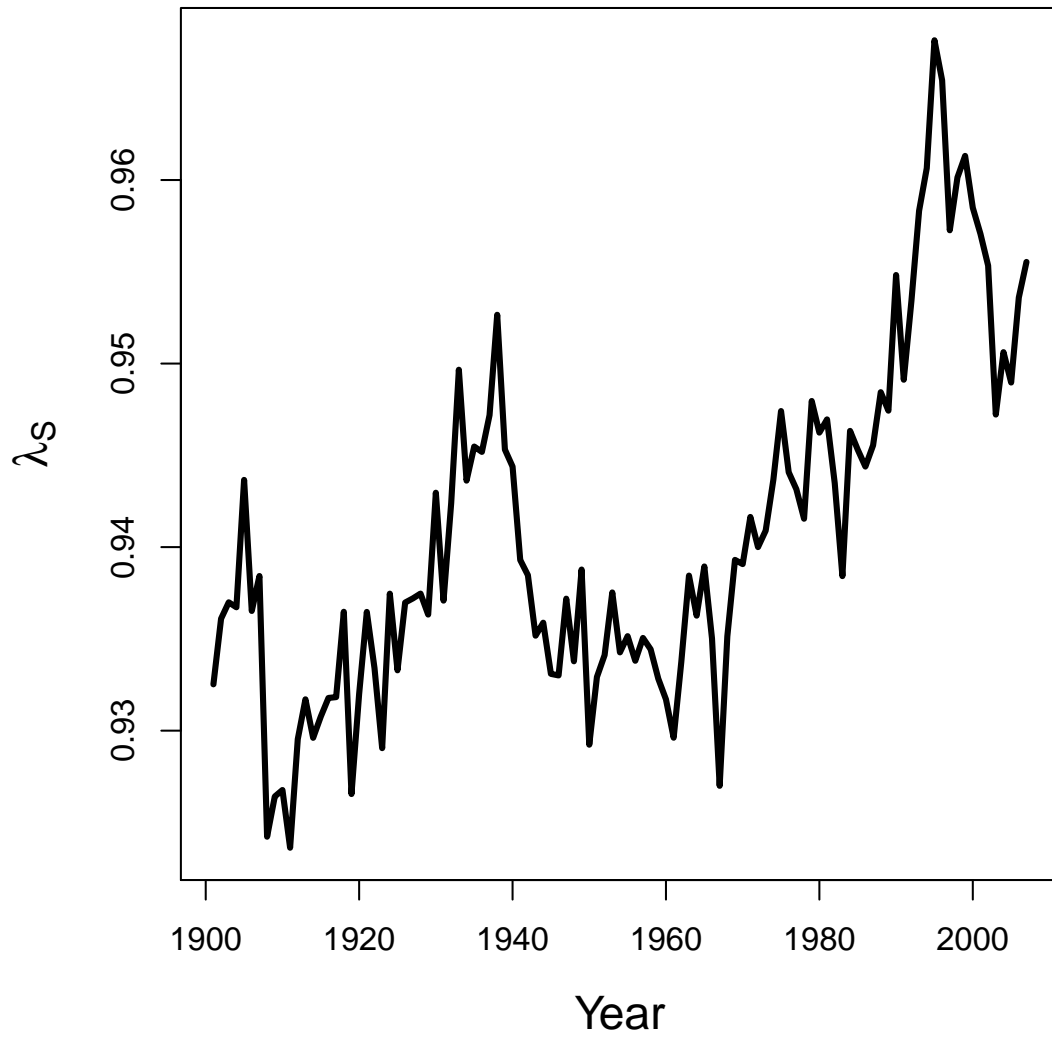


Figure C4: Time series of stochastic population growth rates (λ_S). Values are based on a 10-year sliding window such that λ_S is year t is based on the climate regime over the years t through $t + 9$

862 Appendix D: Exploring the consequences of climate 863 extrapolation

864 Our analysis in the main text relied on extrapolating demographic responses to
865 climate into climate environments that were not directly observed during our field
866 study. For example, high values of PC1 and low values of PC2 were under-
867 represented during the study years (Fig. D1). We explored the consequences
868 of this extrapolation by re-running our demographic analysis with bounds on cli-
869 mate responses. For each vital rate that responded to a climate PC according to
870 some function $f(PC)$, we defined a second function $f^*(PC)$ as:

$$f^*(PC) = \begin{cases} f(PC_L), & \text{if } PC < PC_L \\ f(PC_U), & \text{if } PC > PC_U \\ f(PC), & \text{otherwise} \end{cases} \quad (\text{D1})$$

871 where PC_L and PC_U are the lower and upper bounds, respectively, of the observed
872 range of PC values. For simulations into historical climates more extreme than
873 observed, this approach pins demographic responses to equal the responses at
874 observed extrema, as can be seen in λ responses to PC variation. We repeated our
875 back-casting analysis using this approach.

876 Results show that our qualitative results are not affected by climate extrapola-
877 tion. The back-casted time series of λ was generally consistent with and without
878 extrapolation (Fig. D3). The main differences were in the extreme low λ values,
879 which were lower with extrapolation. Both time series yielded a positive temporal
880 trend, though the mean change in λ per year was 35% weaker for the entire time

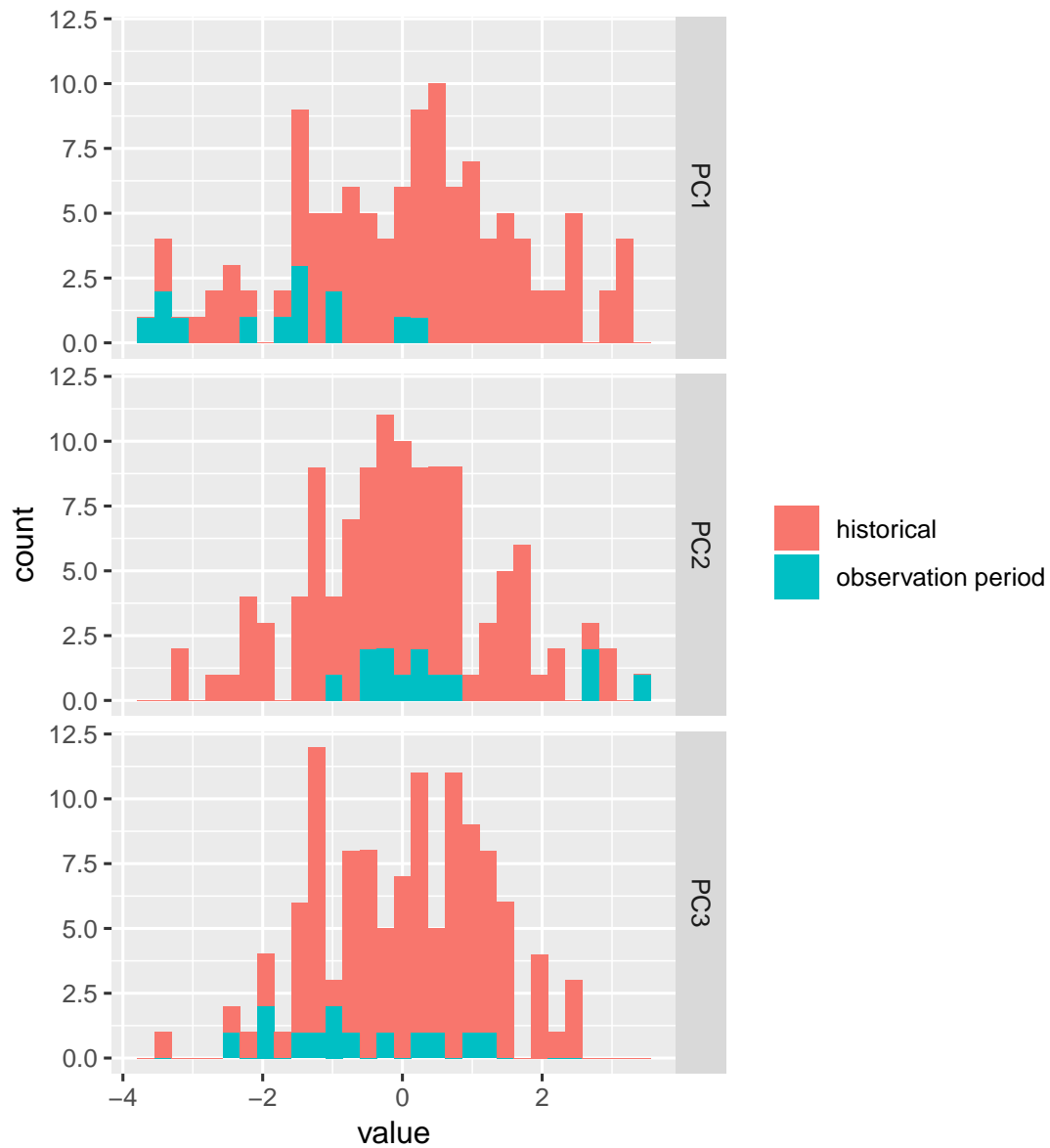


Figure D1: Distributions of observed climate values during the observation period (2004–2017) relative to historical values (1901–2016). Climate values are three principal components of inter-annual variation in cool- and warm-season temperature and precipitation.

series and 26% weaker since 1970 when vital rates were not extrapolated (Fig.
D2). The limited influence of extrapolation was due to the fact that we relied

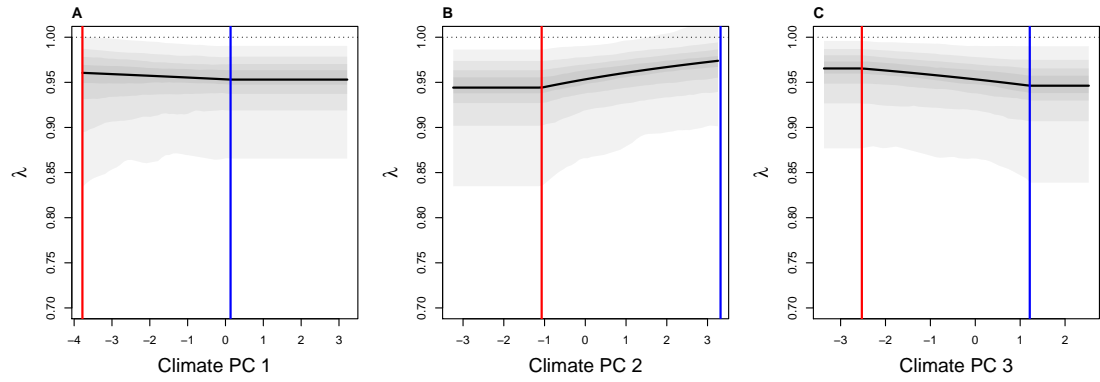


Figure D2: Relationships between λ and three climate PCs with no extrapolation into unobserved climate conditions. For PC values lower than the minimum (red vertical lines) and greater than the maximum (blue vertical lines) of the observation period, demographic responses were forced to match the extrema of the observation period according to Eq. D1.

883 most heavily on extrapolation for PC1 (Fig. D1). As we show in the main paper,
 884 this PC has changed the most during the historical record but it had the weakest
 885 effects on cactus demography.

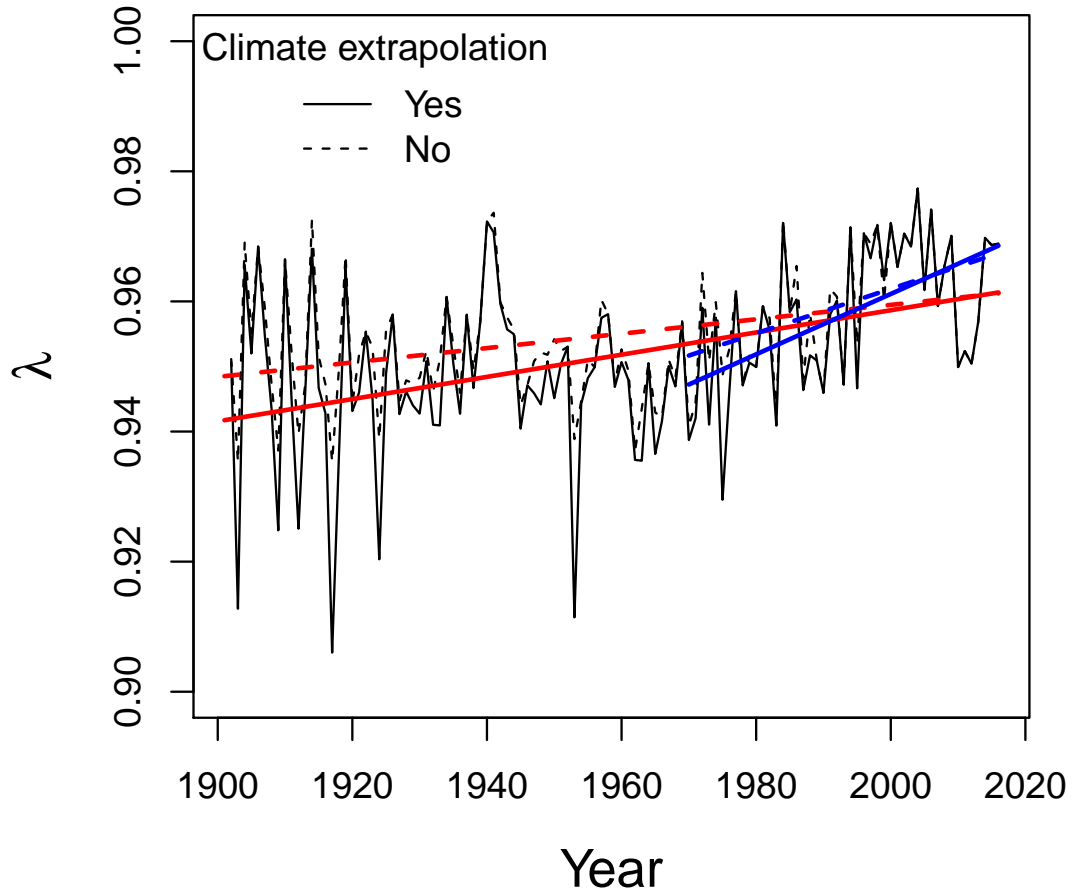


Figure D3: Back-casted values of climate-dependent population growth (λ) with (solid lines) and without (dashed lines) extrapolation of vital rate responses to unobserved climate conditions based on posterior mean parameter values. Red and blue lines show fitted regressions for the entire time series and since 1970, respectively.